



# WPI

## **Evaluation of Subcritical Water Hydrolysis for Sugar Extraction from Malt Bagasse**

A Major Qualifying Project Report

Submitted to the Faculty of

WORCESTER POLYTECHNIC INSTITUTE

In partial fulfillment of the requirements for the

Degree of Bachelor Science in Chemical Engineering

By:

Constantina Eleni Drakontis

Sotirios Filippou

Stephanie Gulezian

Carolyn Morales Collado

Advisor:

Professor Michael T. Timko

# Table of Contents

Table of Contents	2
Table of Figures	4
Table of Tables	6
Acknowledgements	7
Abstract	8
Introduction	9
2. Background	11
2.1 Biomass: A Fuel Resource	11
2.2 Composition of Biomass	12
2.2.1 Feedstock	12
2.2.2 Cellulose	12
2.2.3 Hemicellulose	13
2.2.4 Lignin	14
2.3 Biomass Conversion Technologies	15
2.3.1 Cellulosic Ethanol	15
2.3.1 Anaerobic Digestion	16
2.3.2 Pyrolysis	16
2.3.3 Hydrothermal Processing	17
2.3.3.1 Types of Hydrothermal Processing Techniques	17
2.4 Biofuels	18
2.4.1 Ethanol	19
2.4.2 Biodiesel	20
2.4.3 Bio-oil	21
3. Experimental	22
3.1 Fourier Transform Infrared Spectroscopy	22
3.2 Thermogravimetric Analysis	24
3.3 Batch Reaction	25
4. Results and Discussion	28
4.1 Comparing Extraction Methods	28
4.2 Comparing Flow Rates	29
4.1 Comparing Temperatures	33

5. Conclusions	39
6. Recommendations	40
7. References	42
8. Appendices	48
8.1 Appendix A: FTIR Absorbance Spectra	48
8.2 Appendix B: TGA Results	57

# Table of Figures

Figure 1: Process diagram of biofuel production from biomass.....	10
Figure 2: Structure of cellulose.....	13
Figure 3: Structures of $\alpha$ -D-glucose and $\beta$ -D-glucose.....	13
Figure 4: Structure of xylan.....	14
Figure 5: Structure of lignin.....	15
Figure 6: FTIR diagram [24].....	23
Figure 7: Fitting of DTG curve on Magicplot software.....	25
Figure 8: Untreated malt bagasse used for the batch trials (left) bagasse sample with added water (right). .....	26
Figure 9: Experimental setup of the hot plate.....	27
Figure 10: Samples for 140 °C and 180 °C after batch treatment.....	27
Figure 11: DTG comparison of the 10 mL/min flow rate method vs. the batch method at 160°C.....	28
Figure 12: Absorbance spectrum at 180°C (850cm <sup>-1</sup> - 1800cm <sup>-1</sup> ).....	29
Figure 13: DTG comparison of the 10 mL/min flow rate vs. the 20 mL/min flow rate at 140°C.....	30
Figure 14: DTG comparison of the 10 mL/min flow rate vs. the 20 mL/min flow rate at 210°C.....	30
Figure 15: Absorbance spectrum at 140°C (850cm <sup>-1</sup> - 1800cm <sup>-1</sup> ).....	31
Figure 16: Total concentration of glucose-equivalent total reducing sugars as a function of temperature, at a flow rate of 10 mL/min, retrieved from [58].....	31
Figure 17: Total concentration of glucose-equivalent total reducing sugars as a function of temperature, at a flow rate of 20 mL/min, retrieved from [58].....	32
Figure 18: Concentration of soluble compounds in liquid product vs. hemicellulose extraction.....	32
Figure 19: Concentration of degradation products in liquid product vs. hemicellulose extraction.....	33
Figure 20: DTG comparisons of treatment temperatures for the 20 mL/min flow rate.....	34
Figure 21: Percent composition of 20 mL/min flow rate at varying temperatures.....	34
Figure 22: Absorbance spectrum at the 20 mL/min flow rate (850cm <sup>-1</sup> - 1800cm <sup>-1</sup> ).....	35
Figure 23: DTG comparisons of treatment temperatures at the 10 mL/min flow rate.....	36
Figure 24: Percent composition of 10 mL/min flow rate at varying temperatures.....	37
Figure 25: Absorbance spectrum at the 10 mL/min flow rate (700cm <sup>-1</sup> - 1800cm <sup>-1</sup> ).....	37
Figure 26: The yield of reducing sugars at different S/F as Temperature changes, retrieved from [59]. ...	38
Figure 27: DTG comparisons of treatment temperatures using the batch method.....	38
Figure 28: Absorbance spectrum at the 10 mL/min flow rate (650cm <sup>-1</sup> - 3550cm <sup>-1</sup> ).....	48
Figure 29: Absorbance spectrum at the 10 mL/min flow rate (700cm <sup>-1</sup> - 1800cm <sup>-1</sup> ).....	48
Figure 30: Absorbance spectrum at the 10 mL/min flow rate (2600cm <sup>-1</sup> - 3550cm <sup>-1</sup> ).....	49
Figure 31: Absorbance spectrum at the 20 mL/min flow rate (650cm <sup>-1</sup> - 3550cm <sup>-1</sup> ).....	49
Figure 32: Absorbance spectrum at the 20 mL/min flow rate (850cm <sup>-1</sup> - 1800cm <sup>-1</sup> ).....	50
Figure 33: Absorbance spectrum at the 20 mL/min flow rate (2600cm <sup>-1</sup> - 3550cm <sup>-1</sup> ).....	50
Figure 34: Absorbance spectrum at 140°C (650cm <sup>-1</sup> - 3550cm <sup>-1</sup> ).....	51
Figure 35: Absorbance spectrum at 140°C (850cm <sup>-1</sup> - 1800cm <sup>-1</sup> ).....	51
Figure 36: Absorbance spectrum at 140°C (2600cm <sup>-1</sup> - 3550cm <sup>-1</sup> ).....	52
Figure 37: Absorbance spectrum at 160°C (650cm <sup>-1</sup> - 3550cm <sup>-1</sup> ).....	52

Figure 38: Absorbance spectrum at 160°C (850cm <sup>-1</sup> - 1800cm <sup>-1</sup> ).....	53
Figure 39: Absorbance spectrum at 160°C (2600cm <sup>-1</sup> - 3500cm <sup>-1</sup> ).....	53
Figure 40: Absorbance spectrum at 180°C (950cm <sup>-1</sup> - 3550cm <sup>-1</sup> ).....	54
Figure 41: Absorbance spectrum at 180°C (850cm <sup>-1</sup> - 1800cm <sup>-1</sup> ).....	54
Figure 42: Absorbance spectrum at 180°C (2600cm <sup>-1</sup> - 3500cm <sup>-1</sup> ).....	55
Figure 43: Absorbance spectrum at 210°C (950cm <sup>-1</sup> - 3550cm <sup>-1</sup> ).....	55
Figure 44: Absorbance spectrum at 210°C (850cm <sup>-1</sup> - 1800cm <sup>-1</sup> ).....	56
Figure 45: Absorbance spectrum at 210°C (2600cm <sup>-1</sup> - 3500cm <sup>-1</sup> ).....	56
Figure 46: Composition of treated samples at the flow rate of 10 mL/min. ....	57
Figure 47: TGA results for untreated feed and treated samples at the flow rate of 10 mL/min. ....	57
Figure 48: TGA results for untreated feed and treated samples at the flow rate of 20 mL/min. ....	58
Figure 49: TGA results for treated sample at a flow rate of 10 mL/min and batch experiment at 140°C. .	58
Figure 50: TGA results for treated sample at a flow rate of 10 mL/min and batch experiment at 180°C. .	59
Figure 51: TGA results for treated samples at flow rates of 10 mL/min and 20 mL/min respectively, at 160°C.....	59
Figure 52: TGA results for treated samples at flow rates of 10 mL/min and 20 mL/min respectively, at 180°C.....	60
Figure 53: TGA results for treated samples at flow rates of 10 mL/min and 20 mL/min respectively, at 210°C.....	60

# Table of Tables

Table 1: Types of Biofuels [59] .....	19
Table 2: Characteristic positions of absorbance peaks for FTIR. ....	23
Table 3: Peak fitting of DTG. ....	25
Table 4: Feedstock and water mass used for each batch trial. ....	26

# Acknowledgements

We thank everyone who helped us throughout our Major and Qualifying Project. We thank Daryl Johnson for the training he provided on Thermogravimetric analysis (TGA) and Fourier Transform InfraRed (FTIR). In addition, we thank Maksim Tyufekchiev for his help with the batch experiments and the feedback he provided on the liquid samples. We thank the Unicamp team in Brazil for providing all samples necessary for our experiments. We also thank Geoffrey Tompsett for his guidance and advice as to how to address our results, experiments, and overall assistance in our project. Finally, we thank Professor Timko for advising us throughout the project, his continuous support and guidance with any issues that arose.

# Abstract

The goal of this project was to determine the optimal conditions for sugar extraction from malt bagasse. Our collaborators in Unicamp treated malt bagasse using a semi-continuous flow reactor at two flow rates, 10 mL/min and 20 mL/min, and at four temperatures each, 140 °C, 160 °C, 180 °C and 210 °C. We also treated malt bagasse using a batch process at 140 °C, 160 °C, and 180 °C. Their analysis of the extracted liquid samples suggested that higher flow rate and temperature generated greater sugar yield. To confirm their results, the solid residues were analyzed using Fourier Transform Infrared Spectroscopy and Thermogravimetric Analysis to evaluate their compositions. We concluded that the highest amount of hemicellulose was extracted at the flow through process at a 20 mL/min flow rate and 210 °C.

# Introduction

Wasteful food practices is aiding to the loss of useful resources and world hunger. Food loss and food waste are two terms used to describe any goods that were produced for consumption, but are eventually “discharged, lost degraded or contaminated” [16]. While food loss directly relates to low quantities, food waste describes “discarding or alternative (non-food) use of food that is safe and nutritious for human consumption along the entire food supply chain” [14]. This means that even though the food is produced, it is not used efficiently and is wasted at some point during the production, retail, or consumption stages.

In United States nearly 61 million tons of food waste is generated every year [8]. A study from the journal of Environmental Science and Technology concluded that more food than necessary gets produced. A lot of excess food is being wasted, instead of being put to use. In America particularly, approximately 40% of all food is thrown out [8]. Not only is food wasted due to spoilage, but is wasted due to insignificant problems such as minor impurities or deformations. Food that is thrown out at the production level is usually viable food that is seen as imperfect, and unworthy of sale [8]. This large percentage of waste adds up to around \$165 billion of wasted produce per year [17]. This food could be put to use in a variety of ways, saving not only money, but energy, and possibly lives. To grow crops, large amounts of water and fertilizer is needed. By throwing away large amounts of produce, water and resources are also being thrown away. Not only is this wasting resources and money, but this produce is being wasted where it could be used for feeding the hungry or help solve the energy crisis.

The causes of food losses and waste in developed countries relate mainly to consumer behavior and lack of coordination between the various actors in the supply chain [18]. Food waste can be compared to a cycle because farmers will not harvest food that isn't perfect because grocers won't buy it because consumers won't choose it. Grocers who throw away food are making a purely economic choice, by making room for fresher, prettier products that will sell better. On a consumer level, inadequate planning and expiry of “best before dates” leads to large amounts of waste, combined with the at-times careless attitude of consumers. While this may be known as a common bad behavior of developed countries, developing countries show an alarmingly similar pattern of food waste [18]. The substantial difference between the two is in the origin of food waste generation. The causes of food losses and waste generation in low-income countries are mainly linked to financial, managerial and technical limitations in harvesting techniques, storage and cooling facilities in difficult climatic conditions, infrastructure, packaging and marketing systems [16].

Food waste is usually landfilled or incinerated, which causes more environmental and economic stress [28]. Some of the problems with this includes the increase in pollution, bacterial contamination, disposal management problems, and varying pH and chemical composition of the soil and water [34]. This has become a worldwide issue as the landfills continue to fill up and the process of incineration continues to cause harm to the environment. New technologies are being developed to expand and utilize the food waste rather than to incinerate or place it into landfills.

The organic and nutrient filled composition of the food wastes that enter landfills makes an excellent resource for biofuel production through fermentation. Fermentation is a chemical process which uses cells to break down sugars for energy when there is a lack of oxygen. Biofuel is defined as any solid, liquid, or gaseous fuel that is made from any renewable source which can include animal fats, biomass, and food waste and its production process from biomass can be seen on Figure 1. The benefits to biofuel is that it does not produce as big of a carbon emission when it is utilized in comparison to fossil fuels [32]. The growing demand for alternative sources of fuel to replace petroleum and coal has made biomass fuel alternatives a promising source of energy.

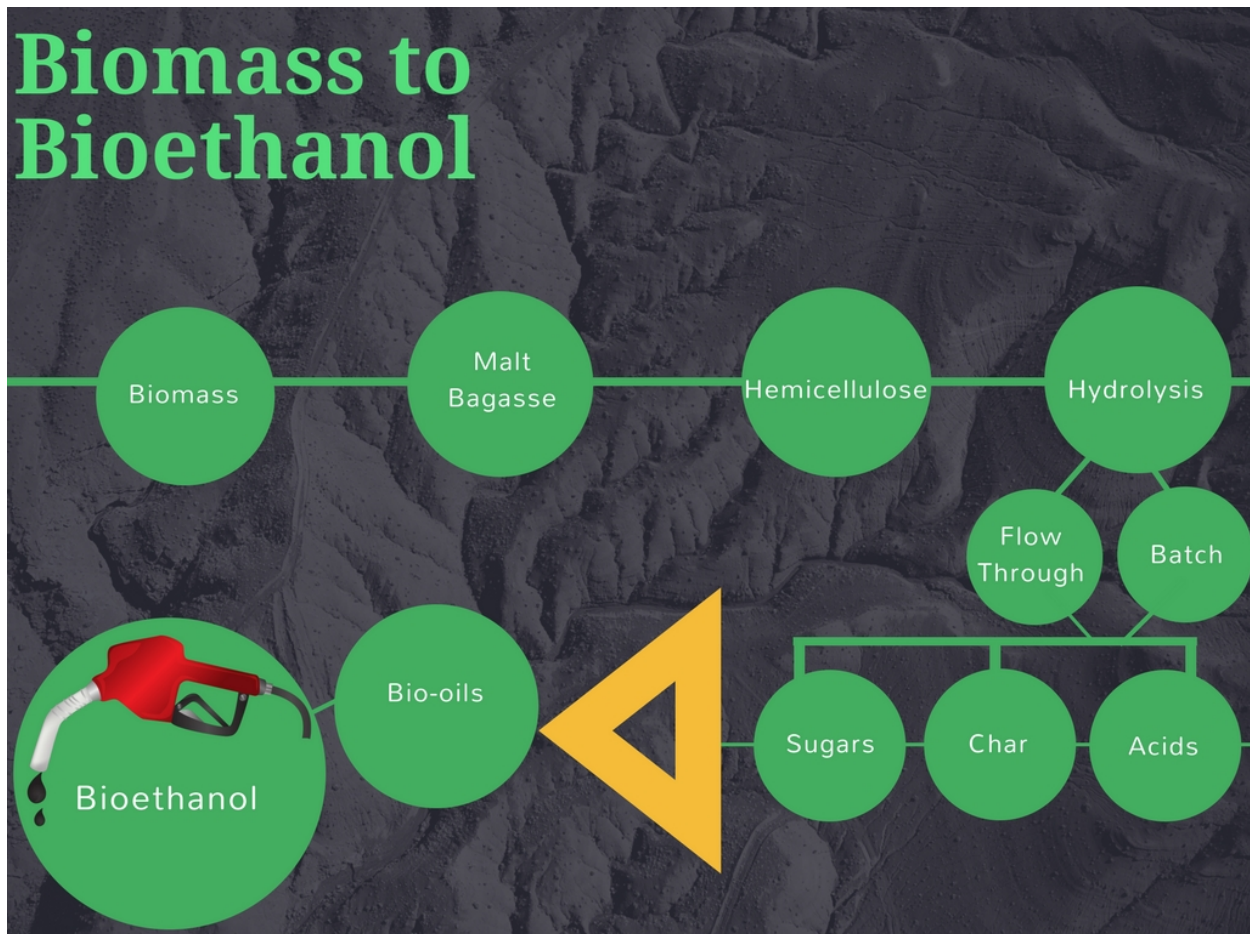


Figure 1: Process diagram of biofuel production from biomass.

## 2. Background

### 2.1 Biomass: A Fuel Resource

Biomass refers to substances derived from organisms, such as plants and animals [5]. Biomass is characterized as a natural and renewable resource. Renewable natural resources are identified as naturally occurring materials and substances that can be exploited for economic benefits and have the ability to naturally replenish in an equal or a shorter period of time when consumed [5]. Historically, biomass has been utilized to produce heat, steam and power, and bioenergy-energy generated from biomass- could be used to cover part of the high energy demand of today's society [26].

The energy stored in biomass originates from solar energy. Plants use the energy from the sun and the carbon dioxide that exists in the atmosphere to convert it to glucose, releasing oxygen via photosynthesis. This carbon is then transferred to other organisms, such as animals and microorganisms, through food chains until it biodegrades. It returns to the atmosphere in the form of carbon dioxide (CO<sub>2</sub>) or methane (CH<sub>4</sub>), depending on whether the conditions are aerobic or anaerobic [5]. Consequently, the CO<sub>2</sub> is again available for the production of biomass. This is the cycle of carbon in the atmosphere [46].

The benefit of using biomass as a fuel against fossil fuels is that biomass does not add a new amount of carbon dioxide in the atmosphere. Fossil fuels, like coal and oil, originate from fossil biomass, which requires millions of years to be composed, and the rate of addition of carbon dioxide to the atmosphere is quite small relative to the one of its consumption. However, using biomass as fuel does not charge the atmosphere with excess carbon dioxide, a greenhouse gas, since it would naturally return as carbon dioxide to the atmosphere due to biodegradation [46].

Liquid or gas fuels generated from biomass are defined as biofuels [52]. Biofuels are classified into three categories: first-generation, second-generation and third-generation biofuels based on their source. The raw material for the first-generation biofuels is biomass appropriate for consumption (oils, sugars, starches), for the second-generation ones biomass that is not edible (grasses, woody materials etc.), and for the third generation ones algae [31].

The biomass originates from a variety of resources, such as dedicated energy crops, agricultural crop residues, forestry residues, algae, wood processing residues, municipal waste, and wet waste [60]. A relatively untapped resource for biofuel generation is wasted food. Food waste per capita for developed countries is 107 kg/year and 56kg/year for the developing countries [13][57]. This shows a large problem of wasted resources. A large contributor to food waste is the food manufacturing industry. With leftovers from food processing, ie. orange peels from a juice factory, being currently unused, the potential for food waste to be utilized for the production of biofuels is a great solution to a growing problem.

## 2.2 Composition of Biomass

### 2.2.1 Feedstock

Malt bagasse is a renewable plant biomass source with a low cost, generated in large quantities as a residue from beer production and can be used in different applications of bioprocessing. Bio-oils obtained from plant biomass such as malt bagasse, are commonly used as raw materials for the production of biodiesel [63].

The main component of a plant biomass is lignocellulose [2]. Cellulose and hemicellulose compose the carbohydrate section of the biomass (carbohydrate polymers), while lignin formulates the non-carbohydrate section (aromatic polymers). The interactions and bonds between the three components make it hard for them to be separated and processed into biofuels, as an alternative and sustainable energy choice. The structural and mechanical strength of the plant are due to cellulose and hemicellulose, whereas the stability of its structure is due to lignin surrounding the other two [41].

In order to generate a biofuel from the biomass, lignocellulose has to be decomposed. Glucose is a monosaccharide that composes cellulose and hemicellulose. Glucose can easily be processed into ethanol, which is then easily transformed into an alternative and sustainable fuel source [63]. Even though ethanol is not the only sugar present in the biomass, its yield is greater than the other sugars present [40] making it the best choice for biofuel synthesis from a plant biomass such as barley bagasse.

### 2.2.2 Cellulose

Considering the potential of biomass as a renewable energy resource, the conversion of cellulose from biomass to biofuels has been the center of a lot of research. Cellulose is a symmetric organic compound, structurally the most prominent component in plants [9]. It is a polysaccharide considered nearly inexhaustible and the most abundant natural polymer with about  $1.5 \times 10^{12}$  tons of the total annual biomass production [29]. Cellulose is an important component because it has a great amount of glucose molecules within its structure. It is insoluble in water at room temperature, and it is biodegradable. When treated in hot compressed water, it can be broken down chemically into its glucose units.

Cellulose is composed of repeating glucose units, resulting in various attributes and functions. Its characteristics and interactions depend, amongst others, to the chain length and distribution of functional groups. It is generated by the linkage of  $\beta$ -D-glucopyranose molecules which are covalently linked by the  $\beta$ -1,4-glucosidic linkage. Cellulose has a high degree of polymerization (DP), which depends on the treatment of the feedstock, affecting the total number of the repeating structural units [29]. For example, wood pulp DP values are 300 and 1700 usually,

whereas cotton and bacterial cellulose have values ranging from 800-1000 [29]. The structure of cellulose is shown on the Figure 2 below.

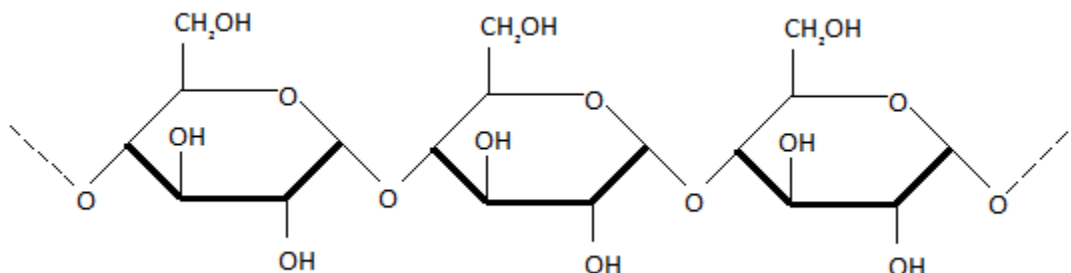


Figure 2: Structure of cellulose.

Glucose can exist in two forms,  $\alpha$ -D-glucose and  $\beta$ -D-glucose [9]. The difference between the two is the position of the substituent at the anomeric center. As shown below, in  $\alpha$ -D-glucose the exocyclic oxygen group is on the opposite face to the  $-\text{CH}_2\text{OH}$  group, whereas in  $\beta$ -D-glucose it is on the same face. The importance of the two different structures lies in the easiness to be broken down. More specifically,  $\beta$ -D-glucose rings form cellulose whereas  $\alpha$ -D-glucose rings form starch. Starch is broken down much easier than cellulose, which is due to the different structures of the two glucose isomers.

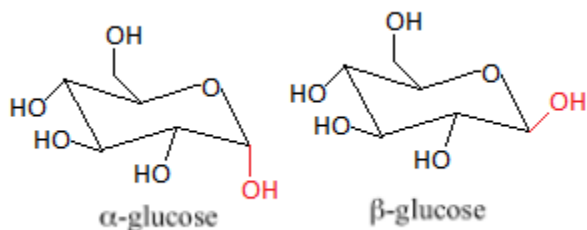


Figure 3: Structures of  $\alpha$ -D-glucose and  $\beta$ -D-glucose.

### 2.2.3 Hemicellulose

Hemicellulose is also a component of biomass. It has a similar structure to cellulose in terms of having the  $\beta$ -D-glucose ring, but it is composed of various different sugar units, such as xylan and glucomannan [4]. The sugars are arranged in different proportions including different substituents.

The degree of polymerization of hemicellulose is around 100-200 sugars per molecule, which is much lower than cellulose (10000 sugars per molecule) [47]. Due to its asymmetric structure and high branching, it is less stable than cellulose. This makes it easier to break down the molecule and it degrades with heat treatment. Hemicellulose forms hydrogen bonding with cellulose, while it bonds covalently with lignin, which surrounds it. Xylan is an example of a typical hemicellulose structure, and can be found below.

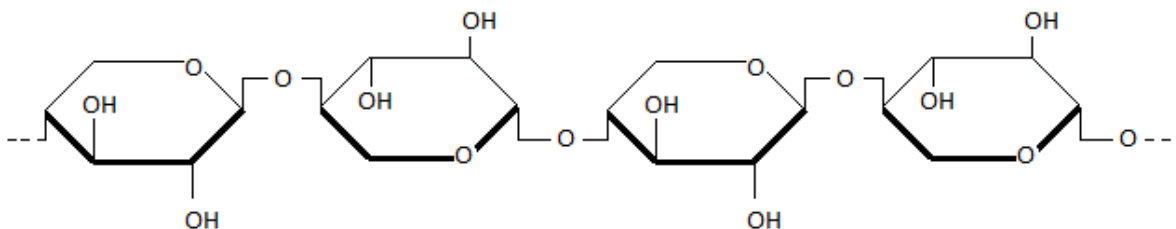


Figure 4: Structure of xylan.

#### 2.2.4 Lignin

As mentioned above, lignin is a major component of plant biomass, and more specifically in our case with barley bagasse. Just as with cellulose and hemicellulose, we are interested to see how the process of the feedstock affects the amount of lignin present in our samples. Lignin essentially consists of integrated aromatic substances, which are arranged nonspecifically [36]. It contains both hydrophilic and hydrophobic groups, but its hydrophobic character is more prominent resulting to its low solubility in water [62]. Its structure is more complex than that of cellulose and hemicellulose described previously, as seen on the figure below.

Lignin does not obtain a single prominent structure and its composition changes from case to case, making it possible to define it by its heterogeneity. It is also considered a complex polymer because its structure changes according to the feedstock biomass. Due to its higher energy content, it provides a biomass with a higher heating value in comparison to cellulose and hemicellulose. It is also the reason why aggressive hydrolysis conditions must be used to isolate glucose molecules [62]. Plants use lignin to help strengthen their structure, regulate the flow of fluids, store energy and protect against microorganisms. Specifically in wood, lignin encloses cellulose and hemicellulose, making it harder to break the molecules down by hydrolysis [35].

Regarding the decomposition of lignin, only certain species have the enzymes needed in order to degrade it successfully [36]. Its degradation also becomes more difficult due to its resistance to being broken down by thermochemical and biological processes. This makes its removal from biomass a costly process, which is why a lot of research is put into designing plants that either deposit less lignin or produce more lignin that is responsive to chemical degradation. Its structure also has a significant impact on product yields and products during hydrothermal

processing, making it more resistant to natural decay and biological degradation [35]. Lignin is one of the most prominent limiting factors in the conversion from biomass to biofuels, since it protects cell wall polysaccharides from degrading. In addition, not much is known about degradation under hydrothermal liquefaction, a thermal depolymerization process used to convert biomass into bio-oil.

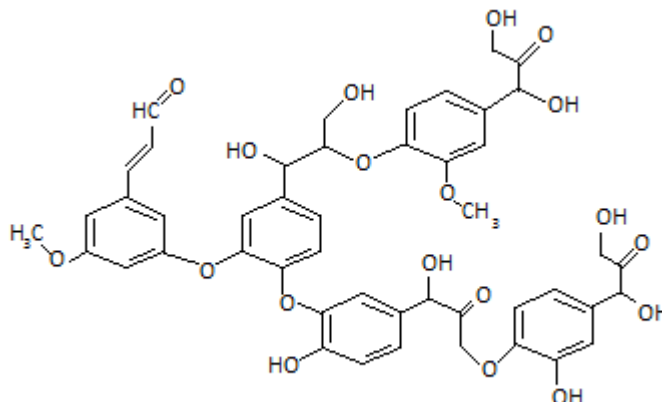


Figure 5: Structure of lignin.

## 2.3 Biomass Conversion Technologies

A variety of process for the production of fuels from biomass can be found in literature. In this section, three of the most common types of such process are introduced, anaerobic digestion, pyrolysis and hydrothermal processing. Additionally, three specific hydrothermal process are described, as this is the focus of our study.

### 2.3.1 Cellulosic Ethanol

Lignocellulosic biomass, such as forest and agricultural residues, wood products and animal and human wastes, can be used for the production of fuel ethanol. The advantage of this type of biomass against starch (e.g. corn) and sucrose (e.g. sugarcane) is that it is less expensive [67]. These materials are abundant and can be used for manufacturing biofuels without extra land requirements or affecting the food and fiber crop production. As a result, not requiring edible biomass a source, cellulosic ethanol is characterized as a second generation biofuel [50]. Cellulosic biomass can be transformed into biofuel through biochemical or thermochemical processes. However, combination of both processes is more effective [20].

The biochemical process consists of three steps, pretreatment, hydrolysis, and fermentation [67]. Pretreatment is the step where the lignin-carbohydrate complex that encloses the cellulose and hemicellulose is disordered to allow access to enzymes. There is a variety of technologies that

can be used for pretreatment and can be divided into biological, chemical, physical and thermal processes [65]. For effective hydrolysis, pretreatment is necessary. In hydrolysis, released polysaccharides break down into monosaccharides. Afterwards, naturally occurring or genetically modified microorganisms ferment these monosaccharides into ethanol [67].

The thermochemical processes, such as gasification and pyrolysis, involve heating biomass without or with limited oxygen to generate biofuel or other products. In gasification, the feedstock is heated with the presence of the one-third of the required oxygen for combustion and syngas, a mixture of carbon monoxide and hydrogen, is produced. Syngas can be utilized as a fuel or converted to other fuels and chemicals. Pyrolysis is a similar process but with the absence of oxygen. From pyrolysis, a bio-oil is generated that also can be utilized as a fuel or converted to other fuels and chemicals [20].

### 2.3.1 Anaerobic Digestion

Anaerobic digestion is a biological process where a microbial consortium decomposes carbonaceous matter in the absence of oxygen to generate biogas [33]. Biogas consists primarily of methane and carbon dioxide as well as some other gases, for example hydrogen sulfide, in smaller amounts [11]. The anaerobic digestion occurs in airtight containers named digesters [43].

Decomposition of organic matter happens in four successive stages. First, complex polymers break down into monomers with the help of enzymes in a process called hydrolysis. Afterwards, acidogenesis takes place and the monomers are converted to volatile fatty acids and hydrogen. The next step is acetogenesis where the volatile fatty acids react to generate acetate, carbon dioxide, and hydrogen. Finally, the acetate is converted to methane during methanogenesis [43].

Several factors influence the rate of digestion and biogas production, but the most significant one is temperature. The microorganisms responsible for digestion can survive temperatures between below 0°C and 57.2°C; however they perform best at 36.7°C (mesophilic) and 54.4°C (thermophilic). The rate of digestion decreases greatly at temperatures in the range of 39.4°C and 51.7°C and 0°C to 35°C [11].

### 2.3.2 Pyrolysis

Pyrolysis as well as liquefaction and gasification are thermal degradation processes [39]. Pyrolysis transforms biomass or other feed to a variety of solid, liquid, or gaseous products by heating it, without the presence or with a limited supply of oxidizing agents, at a defined rate until reaching a maximum temperature (pyrolysis temperature) and keeping it in this condition for a particular time period. The quality of the product depends on the process variables, such as the pyrolysis temperature, heating rate, and residence time [4].

Generally, the process of pyrolysis involves six steps. First, the fuel is heated using a heat source. As the temperature raises, primary pyrolysis reactions occur producing volatiles and char. Hot volatiles start flowing and heating up solids with lower temperature. Part of the volatiles condensate on the lower temperature portions of the fuel and secondary reactions take place

resulting in the formation of tar. Primary and secondary pyrolysis reactions, mentioned above, take place at the same time. Lastly, there is the possibility of “further thermal decomposition, reforming, water gas shift reaction, radicals recombinations, and dehydration” based on the process parameters [39].

### 2.3.3 Hydrothermal Processing

Hydrothermal processing or “Hydrothermal Upgrading (HTU<sup>®</sup>)”, a method for biomass conversion, was proposed by the Shell Oil Company in the 1980s. In this process, the mass decomposition occurs in water [56]. Subcritical or supercritical water at increased temperature (regularly 200-800°C) and pressure (regularly 5-30 MPa) is used as the medium [53]. The major advantage of this technology against the rest of biomass conversion methods is that wet biomass can be processed as the feedstock. Most types of biomass contain considerable amount of moisture, and drying the feedstock is an extra procedure with added cost in industrial applications [53].

Changing the operating conditions, i.e. temperature and pressure, influences the properties of water, and as a result, the biomass reactions. The most significant properties for this technology are miscibility, density, dielectric constant, ionic product, hydrogen bonds, viscosity, and diffusion coefficients. By exploiting these properties, water can function as solvent, reactant, and catalyst [53].

#### 2.3.3.1 Types of Hydrothermal Processing Techniques

One method of hydrothermal processing is using a supercritical method. This method uses supercritical fluid at high temperatures and pressures in a continuous process. Superheated fluid flows through the organic product to extract compounds convertible to biofuels. Not only is it catalyst free, but also can tolerate water in the organic produce. Furthermore, it can handle fatty acids, which are broken down into methyl esters [25], allowing for a large range of produce to be able to be processed, unlike the selective tendencies of the catalyst method. Even though this procedure requires extreme pressures and temperatures, it is more cost efficient than catalytic methods [25]. One well known use for this method is the decaffeination of coffee, but this process can be used in pharmaceutical, biomedical, and biofuel industries.

Non-catalytic transesterification is another process in which hazardous catalysts are not used to make biofuels. Unlike the supercritical method, fluids at high temperatures and pressures that are just under the supercritical stage are used. Additionally, the process is done in batches, which provides the benefit of larger productions, but slightly longer times and, in some cases, lower conversions [45].

A third method is a non-catalytic two-step process that requires very high temperatures and high molar ratios of alcohol to oil [30]. This process first uses a hydrolysis step using subcritical water, which splits fatty acids off of the triacylglycerol. Second, the fatty acids undergo a process using supercritical methanol to produce biofuel providing a lot of promise in the biofuel industry. In contrast with the current methods being used, it requires very little refining steps after

production before it can be used. This would make it economically efficient and less wasteful because of the absence of catalyst.

## 2.4 Biofuels

In recent years, fossil fuels are the primary source of energy, and extensively used for transportation. Fossil fuels contribute to a large portion of greenhouse gases, and therefore, biofuels are becoming the best alternative to substitute petroleum-based fuels [42]. During the last 25 years, the global production of biofuels has increased approximately from 4.4 to 50.1 billion liters, and it is expected to follow this pattern in the future [42]. As previously discussed, biofuels are liquid or gas fuels made from biomass and are categorized in first generation, second generation, and third generation. Some examples of biofuels are ethanol, methanol, biodiesel, and biobutanol [59]. Table 1 presents a detailed list of biofuels, examples of biomass they can be derived from, and their energy density.

Table 1: Types of Biofuels [59]

First Generation		
Fuel	Energy Density (MJ/kg)	Feedstock
Ethanol	30	Starches from wheat, corn, sugar cane, molasses, potatoes, other fruits
Propanol	34	
Butanol	36.6	
Biodiesel	37.8	Oils and fats including animal fats, vegetable oils, nut oils, hemp, and algae
Green Diesel	37.8	Made from hydrocracking oil and fat feedstock
Castor Oil	39.5	Unmodified or slightly modified
Olive Oil	39	
Fat	32	
Sunflower Oil	40	
Bioethers		Dehydration of alcohols
Biogas	55	Methane made from waste crop material through anaerobic digestion or bacteria
Wood	16-21	Everything from wood and sawdust to garbage, agricultural waste, manure
Dried Plants	10-16	
Bagasse	10	
Manure	10-15	
Seeds	15	
Second Generation		
Fuel	Energy Density (MJ/kg)	Feedstock
Cellulosic ethanol		Usually made from wood, grass, or inedible parts of plants
Algae - based biofuels		Multiple different fuels made from algae
Biohydrogen	123	Made from algae breaking down water
Methanol	19.7	Inedible plant matter
Dimethylfuran	33.7	Made from fructose found in fruits and some vegetables
Fischer-Tropsch Biodiesel	37.8	Waste from paper and pulp manufacturing

### 2.4.1 Ethanol

Bio-ethanol is an ethyl-alcohol, chemically represented as  $C_2H_5OH$ . Ethanol is derived from various types of feedstock which can be divided in three different groups, sucrose containing biomass, such as sugar cane, sugar beet, and fruit, starch-rich materials, for example corn, rice,

barley, and sweet potatoes, and lignocellulosic biomass such as wood, straw, and grasses [3]. Ethanol production includes the following steps: yeast fermentation, distillation, dehydration, and denaturing. Some feedstock requires saccharification or hydrolysis of carbohydrates [23]. The conversion of sucrose into ethanol is easier in comparison to starch materials and lignocellulosic feedstock because previous hydrolysis of the feedstock is not required since the disaccharide can be broken down by yeast cells [7]. The production of ethanol from starchy materials requires the breakdown of carbohydrate chains to obtain a glucose syrup which can be converted to ethanol by using yeast [7]. In the case of lignocellulosic biomass, pretreatment is required to degrade it and remove the lignin. In addition, the cellulose goes through enzymatic hydrolysis in order to obtain ethanol. The sugars that are released during the hydrolysis can also be converted to ethanol [7].

Ethanol and a mixture of ethanol with gasoline has been used as an alternative of transportation fuel in various countries including France, Germany, United States, and Brazil [3]. Bio-ethanol has a higher octane number than gasoline, broader flammability limits, higher flame speeds, and a higher heat of vaporization. These properties lead to a shorter burn time and higher compression ratio which offer more advantages over gasoline [3]. Ethanol can be used in purer form but in many occasions, it is blended with gasoline in order to produce E10 (10% ethanol and 90% gasoline), E15 (15% ethanol and 85% gasoline), and E85 (85% ethanol and 15% gasoline) [61].

## 2.4.2 Biodiesel

Biodiesel is a biofuel derived from various oils such as vegetable oil, palm oil, sunflower oil, and waste oil [22]. Oils are mixed with an alcohol, for example methanol, and a catalyst, such as sodium or potassium hydroxide [62]. This process is known as transesterification and as a result there are two products, methyl esters and glycerin [12]. The general process consists of three reversible reactions. In the first reaction the triglyceride diglyceride is obtained. Secondly, monoglyceride is obtained from the diglyceride. In the final reaction, glycerin is produced from the monoglyceride [37].

Biodiesel is not composed of petroleum but it can be mixed with a certain percentage of petroleum to produce a biodiesel blend [12]. Diesel engines have shown that when operated on biodiesel there are lower percentages of carbon monoxide emissions and air toxics than when they are operated on a biodiesel blend [37]. In 2003 the worldwide total production of biodiesel was estimated to be 1.8 billion liters [22]. There are many reasons that include its development which include a decrease in dependence on imported petroleum, and its environmental benefits. Biodiesel is renewable and has shown that in comparison to biodiesel blends the emissions of CO<sub>2</sub> were reduced by 78 percent [62].

### 2.4.3 Bio-oil

The liquid product resulting from biomass pyrolysis is known as pyrolysis oil, bio-oil, or bio-crude [67]. Pyrolysis oil is derived from depolymerization and fragmentation reactions of hemicellulose, lignin, and cellulose [67]. Bio-oil has an oxygen content between 35 wt% to 40 wt% [10]. The distribution of oxygen depends on the biomass resources and variables of the pyrolytic process such as temperature, heating rate, and residence time [67]. The level of oxygen is high and as a result the oil has a low density that is lower than 50% in comparison to the conventional fuel [67]. Bio-oil has a major percent of water (15 wt% to 30 wt%) and it also composed of hydroxyaldehydes, hydroxyketones, sugars, carboxylic acids, and phenolic groups [10]. Water lowers the heating value of the bio-oil, delays the ignition rate, and decreases the combustion rate. On the other hand, it reduces the viscosity of the bio-oil and improves fluidity which is ideal for the pumping and atomization of the oil [10]. Bio-oils have an abundance of carboxylic acids, for example acetic and formic acids, which lead to a pH between 2 and 3. Low values of pH make the oil corrosive and hazardous at high temperatures [67].

## 3. Experimental

Our Brazilian collaborators in Unicamp treated malt bagasse using a semi-continuous flow reactor at two flow rates, specifically 10 mL/min and 20 mL/min, and at four different temperatures at each flow rate to extract sugars. The temperatures used in the treatment were 140 °C, 160 °C, 180 °C and 210 °C. To determine the optimal conditions for sugar extraction, the solid residues were analyzed using Fourier Transform InfraRed spectroscopy and ThermoGravimetric analysis. Using these techniques, the amount of sugars left unextracted from the samples was estimated. Furthermore, malt bagasse samples were treated using batch reaction methods at three different temperatures, 140 °C, 160 °C and 180 °C, to compare the batch process with the flow process. Results obtained from FTIR and TGA were also compared to results provided from the team in Brazil.

### 3.1 Fourier Transform Infrared Spectroscopy

The Fourier Transform InfraRed (FTIR) is a method of infrared spectroscopy in which radiation passes through the sample. The sample absorbs part of the infrared radiation while the rest is transmitted. As a result, the spectra represents molecular absorption and transmission. One of the most important facts about FTIR is that no two unique molecular structures produce the same infrared spectrum, which makes it useful for various analysis. The information that can be obtained from the FTIR are identification of unknown materials, determination of quality of samples, and determination of molecular weights of samples in a mixture. Some of the advantages of the FTIR are the speed in which measurements are taken since frequencies are simultaneously measured, it is non-destructive, precise, has less moving parts which reduces likelihood of failure, and produces less levels of noise in the frequencies.

FTIR spectra were obtained using a Bruker Vertex 70 FTIR spectrometer equipped with a La-DTGS detector operated at room temperature. A diamond attenuated total reflectance (ATR) cell, “Golden-Gate” manufactured by Specac, was used for all measurements. For all samples, the resolution was 4 cm<sup>-1</sup>, and 512 scans were acquired and then averaged over the 600–4000 cm<sup>-1</sup> spectral range.

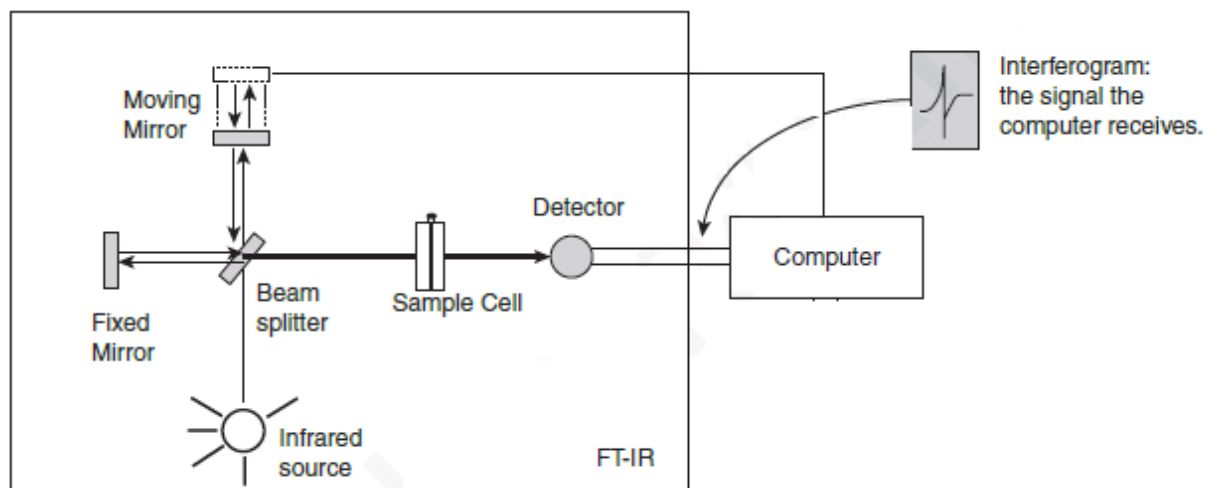


Figure 6: FTIR diagram [24].

After obtaining the absorbance plots of the samples using OPUS software, the specific peaks associated with hemicellulose, cellulose, and lignin were compared to each other at different temperatures, flow rates, and treatment methods. Samples included malt bagasse treated at temperatures of 140°C, 160°C, 180°C, and 210°C. Each sample was tested twice and average values were obtained. In order to determine the components present on the sample, we associated the positions of the main bands to those presented in literature, within a small variation. Table 2 below presents the ranges of values for the positioning of these bands, and how they compare to the values discussed in literature.

Table 2: Characteristic positions of absorbance peaks for FTIR.

Position (cm <sup>-1</sup> )	Position (cm <sup>-1</sup> ) in literature	Assignment	References
897-903	897-910	Cellulose	[27]
1511-1521	1506-1521	Lignin	[1]
1705-1720	1705-1720	Char	[49]
1739-1742	1739-1745	Hemicellulose	[49]

We then compared the relative absorbance and intensities of the absorbances from the samples that have been treated under different temperatures and flow rates. The bands on the FTIR spectra attribute to components of the feed. The main focus was placed on the bands representing

the presence of cellulose, hemicellulose and lignin alongside charring. Most observations were made qualitatively by careful comparison of the amplitude of the bands as well as any shifting in band positions happening. In some cases, where the observations were not as straightforward, a ratio of the amplitudes were considered, in order to standardize our results and get a relative change of the components.

## 3.2 Thermogravimetric Analysis

Thermogravimetric analysis (TGA) measures the rate of change in the mass of a material as a function of rising temperature at constant heating rate, or as a function of time at constant temperature in a controlled atmosphere. From these measurements, the composition of the material based on the thermal stability of the molecules composing the material can be discovered. This technique can show weight loss due to decomposition, oxidation, and dehydration.

TGA was performed under a nitrogen atmosphere using a Netzsch thermogravimetric analyzer (TG 209 F1 Libra). A malt bagasse sample of about 10 to 15 mg was placed into a  $\text{Al}_2\text{O}_3$  crucible previously sanitized over a flame. The crucible was then placed carefully on the thermobalance of the analyzer and the instrument was sealed. The atmosphere surrounding the crucible and sample was then purged with nitrogen gas at a constant rate of 20 mL/min to prevent oxidation or other reactions. The oven temperature was increased from 25 °C to 800 °C at a constant heating rate of 5°C/min.

Since TGA is highly dependent on the temperature range and heating rate, many parameters can interfere with the reaction rate and change the shape of the curve projected. For that reason, we kept the composition of the holder consistent to an  $\text{Al}_2\text{O}_3$  crucible. We also kept the nitrogen flow, the temperature increase rate and starting and ending parameters constant.

The obtained TGA curves were converted in differential thermograms (DTG) using a vendor software. DTG curves were inverted to better observe the changes of magnitude to the lignin, cellulose, and hemicellulose curves. To do this, we plotted the absolute value of the derivative against temperature. Using MagicPlot software, peaks were fit to the DTG curves to determine the peak areas, as presented on Figure 7. To fit the curves, we referenced literature, as seen in Table 3 to estimate the approximate location and size of the curves to get started. Then we manipulated the curves in MagicPlot until the curves represented the data of the DTG curve. The sample composition was estimated from the peak areas. Peak fitting was based on the temperature that each mass component (i.e. hemicellulose, cellulose, lignin, char) decomposes. These values are presented on Table 3.

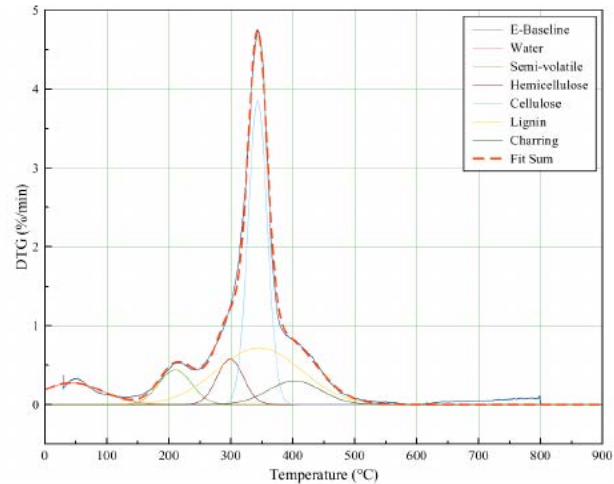


Figure 7: Fitting of DTG curve on Magicplot software.

Table 3: Peak fitting of DTG.

Component	Peak center (°C)	Peak base (°C)	Est. Peak FWHM (°C)	Ref.
Lignin	320-350	150-550	160	[65]
Hemicellulose	283 270-309	175-350	60 40	[44]
Cellulose	330 323-367	280-350	40 40	[15],[6]
Char	400	260-700	100	[15]

### 3.3 Batch Reaction

For extracting sugars from malt bagasse through a batch process, three high pressure glass reaction vials of 15 ml were used. To obtain results comparable to the ones acquired from the already treated samples, the same feed-to-water ratio was used and kept constant as what was used in Brazil's flow through study. The process was repeated at three different temperatures, 140°C, 160°C, and 180°C. Approximately 0.1 g of untreated malt bagasse was measured and placed into each vial while then adding 11.2 ml of water and a 1 cm stir bar (Figure 8). The exact mass of bagasse and water used for each trial can be found below on Table 4.

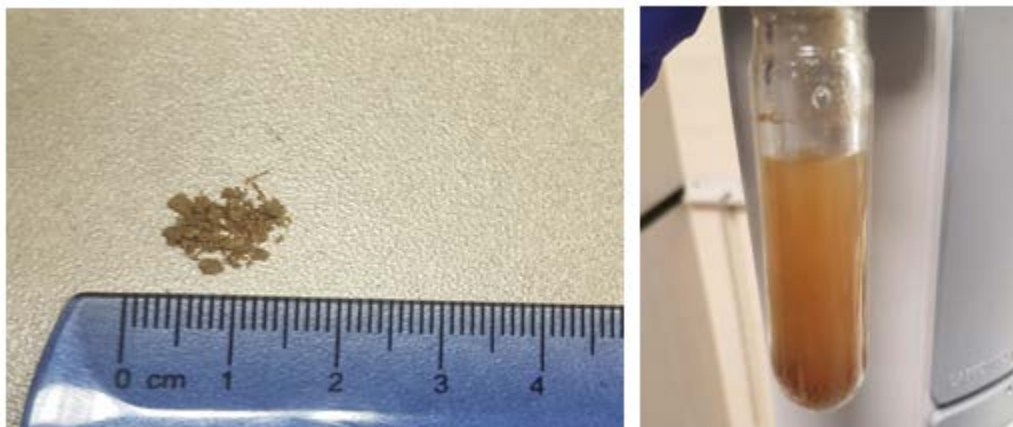


Figure 8: Untreated malt bagasse used for the batch trials (left) bagasse sample with added water (right).

Table 4: Feedstock and water mass used for each batch trial.

Temperature (°C)	Trial	sample mass (g)	water mass (g)
140	T1	0.1167	11.208
	T2	0.1174	11.239
	T3	0.1146	11.211
160	T1	0.1016	11.1905
	T2	0.106	11.204
	T3	0.1013	11.22
180	T1	0.1084	11.2069
	T2	0.1123	11.2175
	T3	0.1108	11.2231

To heat the vials and their contents, a hot plate and an oil bath were used. The hot plate was preheated at the desired temperature (140 °C, 160 °C, or 180 °C) and stirring was set to 200 rpm. After the samples were properly set up, the three vials were submerged in the hot bath assuring they were at the same level of positioning and not touching the bottom of the oil bath since it would affect their temperature. An image of the setup can be found below, on Figure 9. At

the beginning of the experiment, five minutes were timed, until it was ensured the vials were placed properly and they reached the desired temperature. Then, they remained in the bath for 56 minutes. After the total of 61 minutes had concluded, the samples were transferred to a bucket of ice and were left to cool for approximately 10 minutes.



Figure 9: Experimental setup of the hot plate.

To separate the solids from the liquid, filtration flasks and paper were used alongside a vacuum pump. After the liquid product was acquired, the solid residue was rinsed with distilled water and filtered again. Liquid samples were stored at 4° C, whereas the solid residue that remained on the filtration paper was placed in the oven at a temperature of 65° C. Upon dryness, the sample was removed from the filtration paper and stored at room temperature. The liquid products were analyzed through High-Performance Liquid Chromatography (HPLC), while the solid products through FTIR and TGA. Pictures of the final solid product samples can be found below, in Figure 10.



Figure 10: Samples for 140 °C and 180 °C after batch treatment.

## 4. Results and Discussion

### 4.1 Comparing Extraction Methods

In order to compare extraction methods, we used a scaled down batch reaction method at 140°C, 160°C, and 180°C. The instrumentation available was not able to be brought to the final 210°C because it was considered unsafe. The peak at approximately 280°C on the TGA graph in Figure 11 represents hemicellulose. When comparing the batch and flow through methods at 160°C, the amplitude of the peak for batch reaction is higher, meaning that there was more sugar extraction in the flow through method. In the 140°C and 180°C comparisons, as seen on Figures 46-53 in Appendix B, the pattern is the same, showing that there is less hemicellulose present in the flow through samples than in the solid samples of the batch reaction.

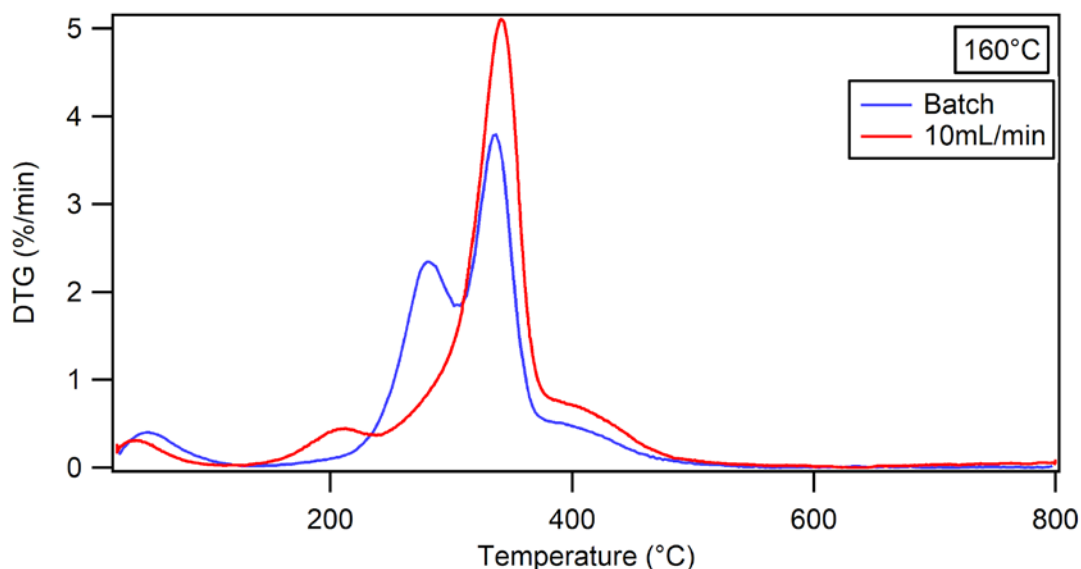


Figure 11: DTG comparison of the 10 mL/min flow rate method vs. the batch method at 160°C

FTIR data was also helpful in order to back up this statement, which can be found in figure 12. Starting with the untreated sample presented on the spectrum below, the broad band at  $899\text{ cm}^{-1}$  is attributed to C-O stretching happening due to the presence of cellulose. The band at  $1514\text{ cm}^{-1}$  is proof of lignin in the sample due to asymmetric aryl ring stretching. Lignin was the material used as a base case when needed to calculate intensity ratios. This is because intensity of lignin is not expected to present a major variation as treatment changes. The band that will be used for comparisons of charring, as treatment temperatures and flow rates vary, is situated between  $1705\text{ cm}^{-1}$  and  $1720\text{ cm}^{-1}$ . As previously mentioned, the positions of the bands vary amongst them slightly. Close ups of all spectra with specific bands and peaks can be found in Appendix A, Figures 28-45.

The strong absorbance band at about  $1739\text{ cm}^{-1}$ , the one to the far right, indicates the presence of hemicellulose in the solid samples and is characteristic of the carbonyl band C=O of hemicellulose. By comparing the amplitude and areas of the peaks for batch and treated feed at  $10\text{ mL/min}$ , we determined that the batch system solid samples contained more hemicellulose compared to the flow-through, meaning there was greater sugar extraction achieved with the flow-through method.

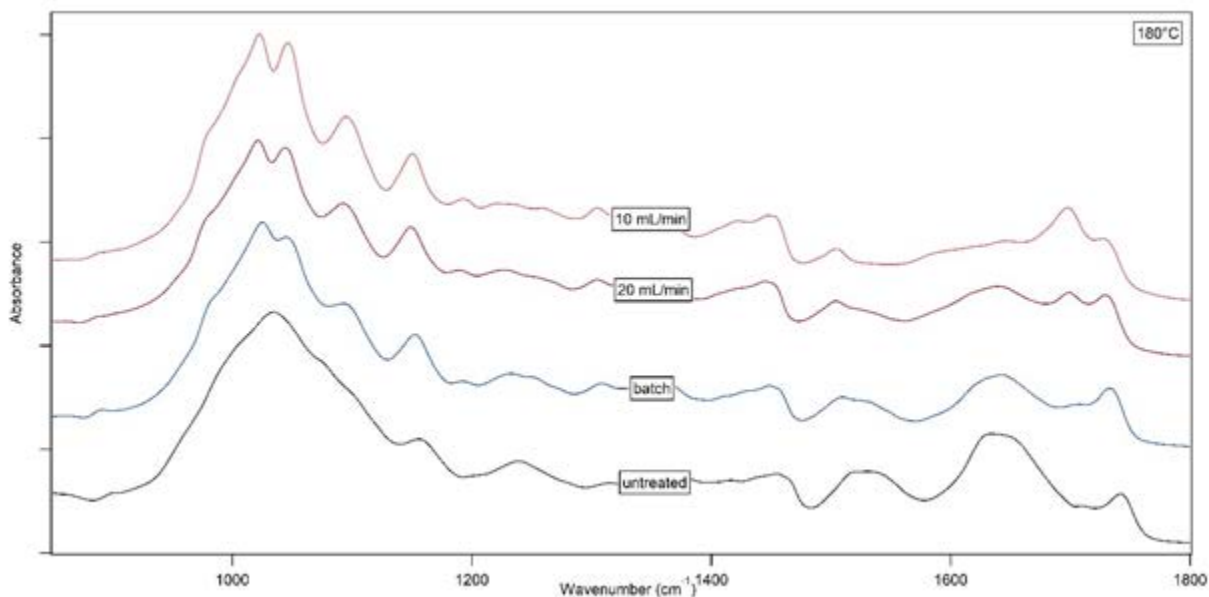


Figure 12: Absorbance spectrum at  $180^{\circ}\text{C}$  ( $850\text{cm}^{-1} - 1800\text{cm}^{-1}$ ).

## 4.2 Comparing Flow Rates

When comparing the two flow rates of  $10\text{ mL/min}$  and  $20\text{ mL/min}$ , the hemicellulose extraction is greater in the  $10\text{ mL/min}$  flow at  $140^{\circ}\text{C}$  and  $160^{\circ}\text{C}$ . At the higher temperatures, the  $20\text{ mL/min}$  flow rate is more efficient. The amplitude of the peak correlates with the larger percentage of hemicellulose in the  $20\text{ mL/min}$  flow, meaning that there was not as much hemicellulose extracted from the sample when compared to the  $10\text{ mL/min}$  flow rate. As shown in Figure 13, the hemicellulose peak in the  $20\text{ mL/min}$  is below the respective one in  $10\text{ mL/min}$  indicating less hemicellulose in the  $20\text{ mL/min}$  sample. Additionally, the amplitude of the peak at around  $350^{\circ}\text{C}$  is significantly larger for the  $20\text{ mL/min}$  than the  $10\text{ mL/min}$  which means that the percentage of cellulose is higher and the percentage of hemicellulose has decreased. In Figure 14, the hemicellulose peak in the  $20\text{ mL/min}$  is more prevalent, showing there is a larger composition of hemicellulose in the sample in this higher flow rate.

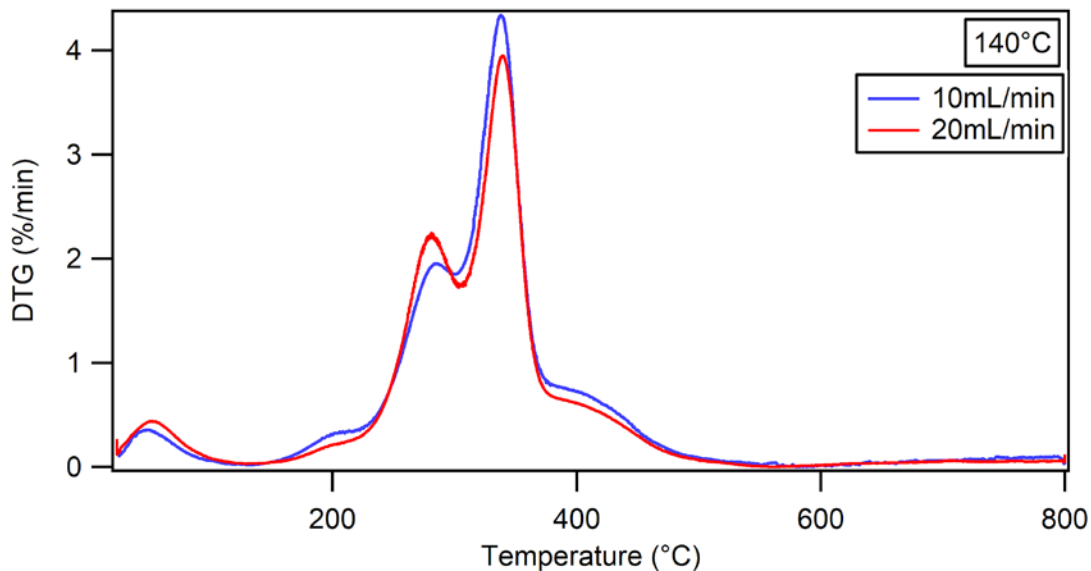


Figure 13: DTG comparison of the 10 mL/min flow rate vs. the 20 mL/min flow rate at 140°C.

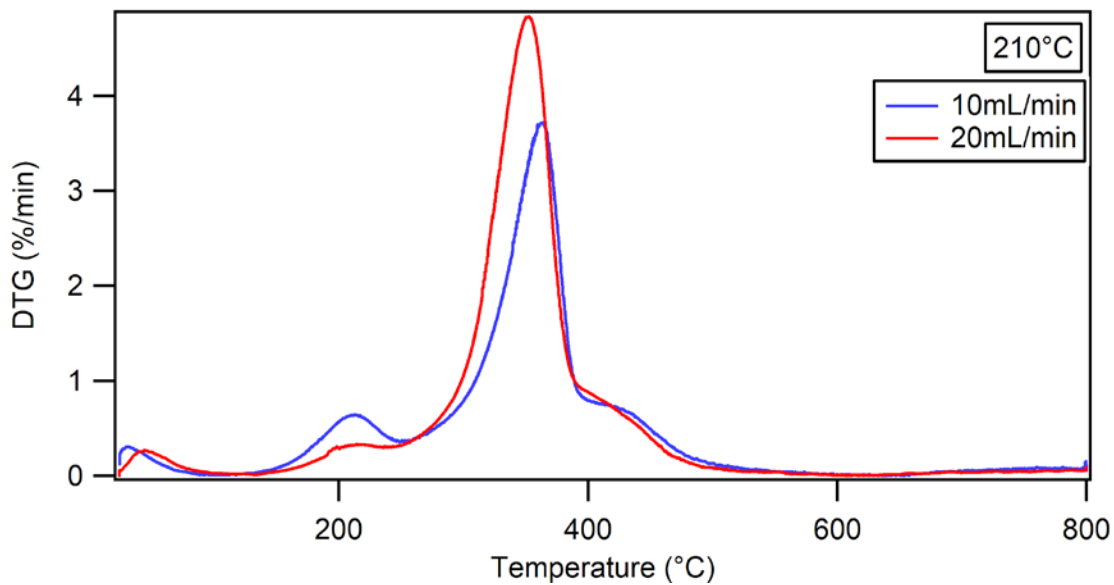


Figure 14: DTG comparison of the 10 mL/min flow rate vs. the 20 mL/min flow rate at 210°C.

In accordance to TGA, FTIR also indicates better sugar extraction at the lower flow rate for the lower temperatures. By comparing the hemicellulose peaks in Figure 15 for the two flow rates, it can be seen that the peak for 10 mL/min is significantly smaller. More hemicellulose has been extracted and thus there is less in the solids left behind.

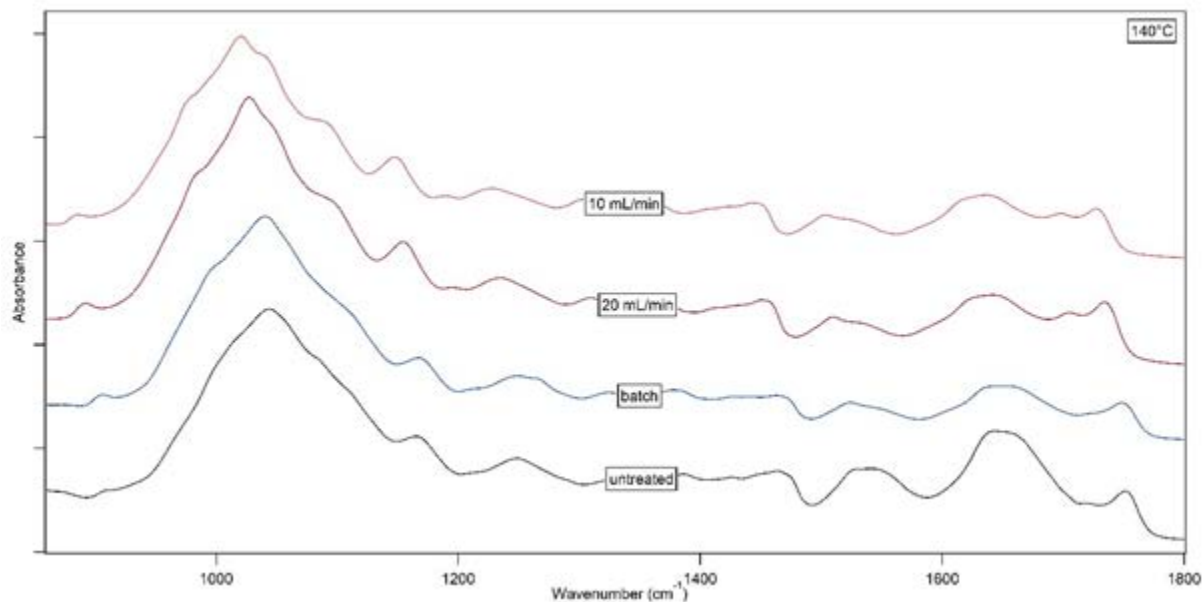


Figure 15: Absorbance spectrum at 140°C (850cm<sup>-1</sup> - 1800cm<sup>-1</sup>).

Most importantly, our data agreed with the complementary data provided by the team in Brazil who analyzed the liquid samples extracted after hydrolysis. Figures 16 and 17 correspond to the 10 mL/min and 20 mL/min flow rates accordingly. By comparing the orange columns (S/F ratio of 64) at 160°C to each other, we see that there is a greater sugar concentration for the 10 mL/min flow rate. However, at the higher temperatures the sugar concentration of 20 mL/min is higher than that of 10 mL/min.

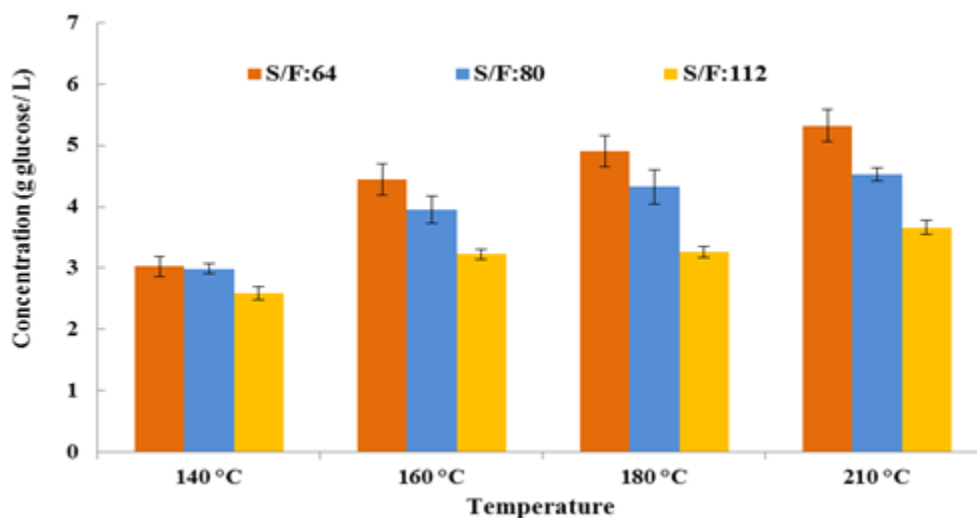


Figure 16: Total concentration of glucose-equivalent total reducing sugars as a function of temperature, at a flow rate of 10 mL/min, retrieved from [58].

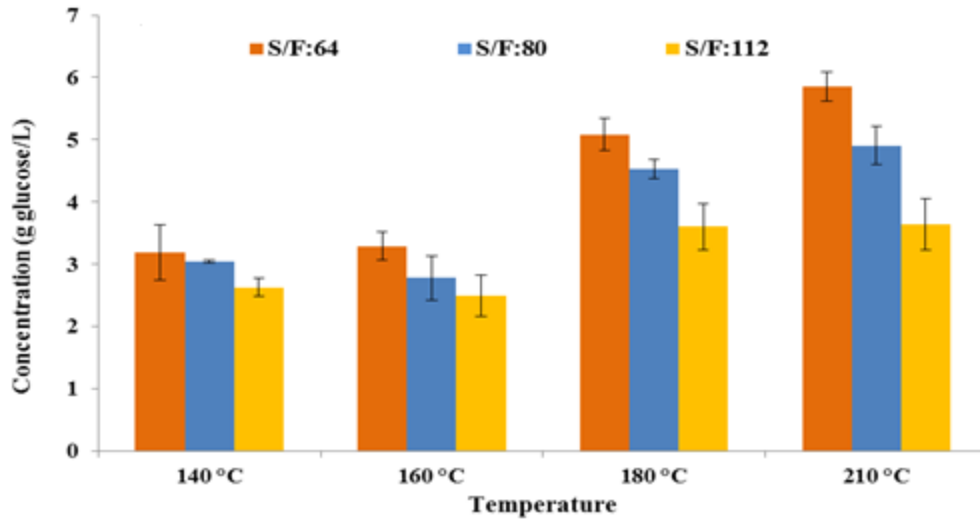


Figure 17: Total concentration of glucose-equivalent total reducing sugars as a function of temperature, at a flow rate of 20 mL/min, retrieved from [58].

In Figure 18 below, it is seen that as more hemicellulose is extracted, there is a higher concentration of soluble products. The soluble products that were detected by the Unicamp group are hydroxymethylfurfural (HMF), furfural, arabinose, galactose, glucose, xylose, fructose, and sucrose.

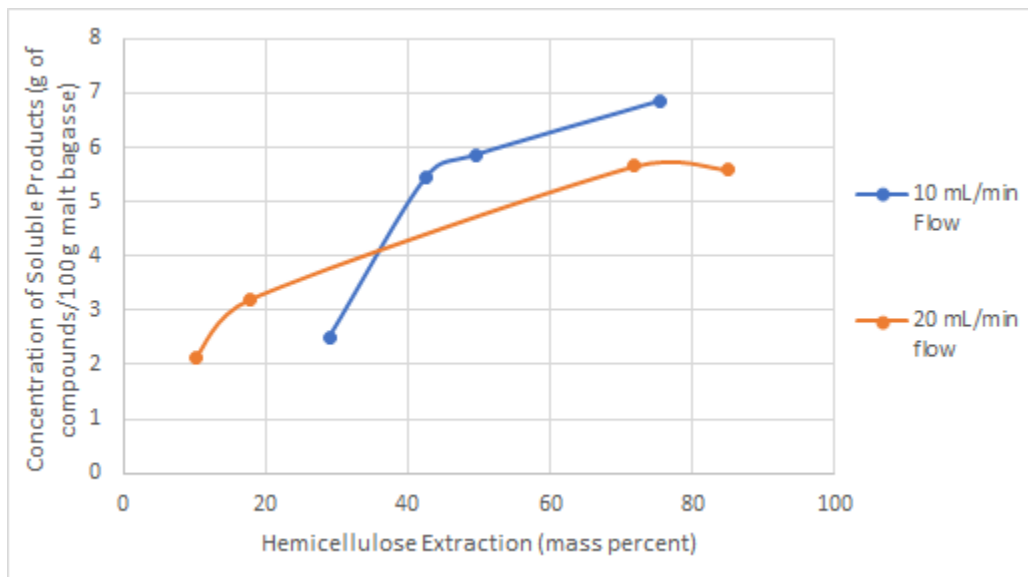


Figure 18: Concentration of soluble compounds in liquid product vs. hemicellulose extraction.

As seen in Figure 19, HMF and Furfural are degradation products, and are observed in the higher amounts as the hemicellulose extraction raises, which is a result of temperature increase.

When comparing the two flow rates to the batch reaction, we used the concentrations of HMF and furfural detected, as they were the only compounds detected in the batch liquid sample. At the 10 mL/min flow rate, the concentration of degradation products is larger than the 20 mL/min flow rate for the higher hemicellulose extraction amounts, in other words for the two higher temperatures (180 °C and 210 °C). The concentration of HMF and furfural also increased in the batch samples, but both compounds were found in significantly low amounts. As a result, we can state that the 20 mL/min is more efficient for these temperatures.

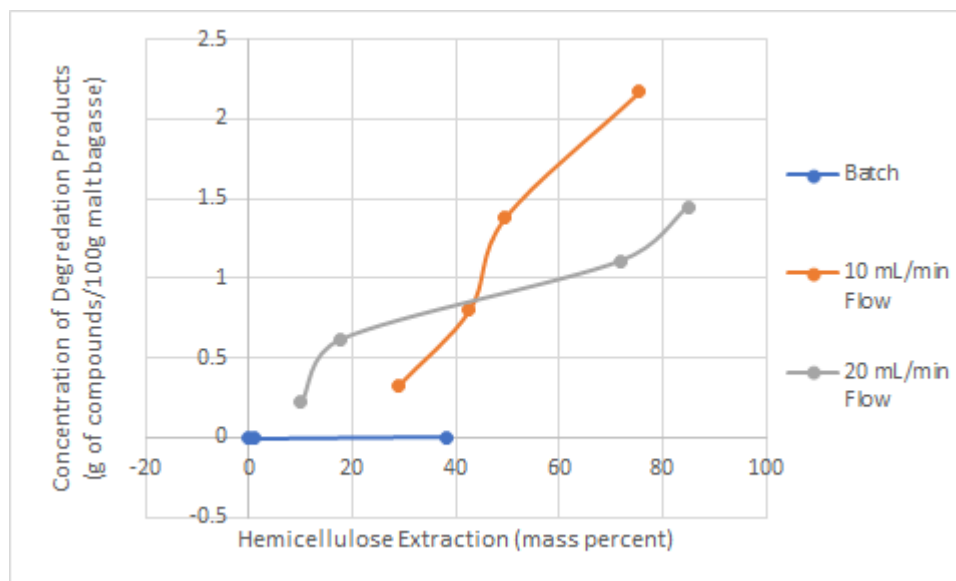


Figure 19: Concentration of degradation products in liquid product vs. hemicellulose extraction.

## 4.1 Comparing Temperatures

Varying treatment temperature had a powerful effect on sugar extraction. The results from the TGA for the samples treated at 20 mL/min flow rate are presented on Figures 20 and 21. As shown in Figure 20, the amplitude of the hemicellulose peak at about 280 °C declines for greater temperatures demonstrating less hemicellulose. Figure 21 displays the composition of the samples as obtained from the peak fitting of the respective DTG curves. The percentage of hemicellulose present in the solid sample is decreasing as the treatment temperature increases. As a result, the amount of sugars extracted at higher temperatures is greater. At 140 °C and 20 mL/min, the percentage of hemicellulose is 27.49% which is smaller by 2.85% from the respective value of the untreated malt bagasse. However, the most drastic decrease occurs from 160°C to 180°C, where it is decreased from 23.83% to 8.47%, and the smallest value (4.48%) is observed at 210°C as seen in Figure 21.

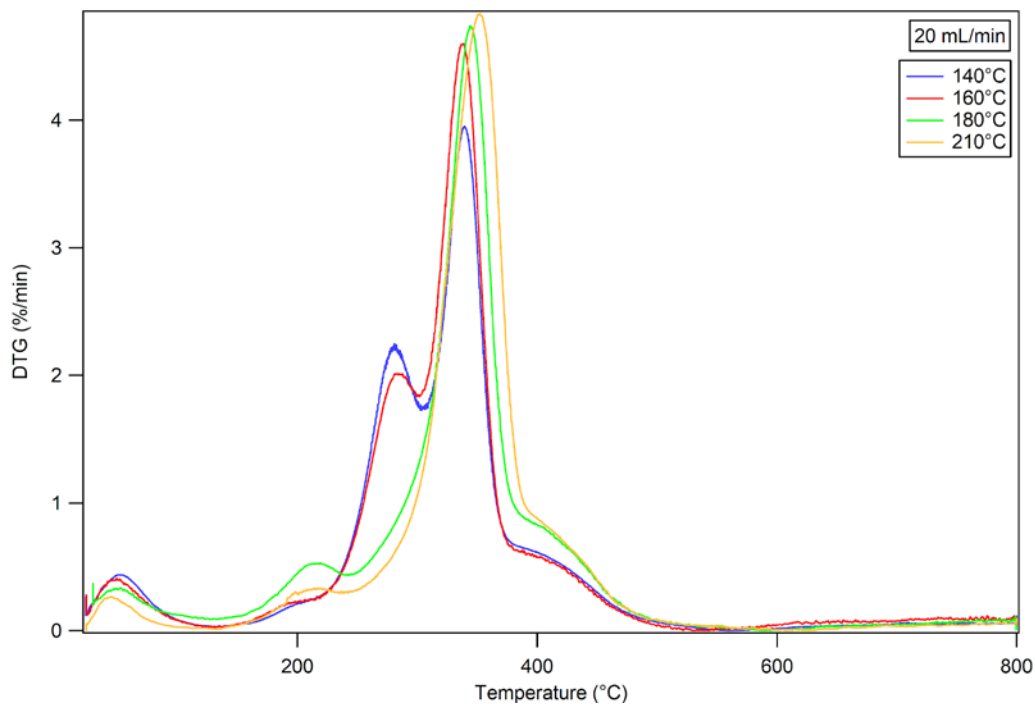


Figure 20: DTG comparisons of treatment temperatures for the 20 mL/min flow rate.

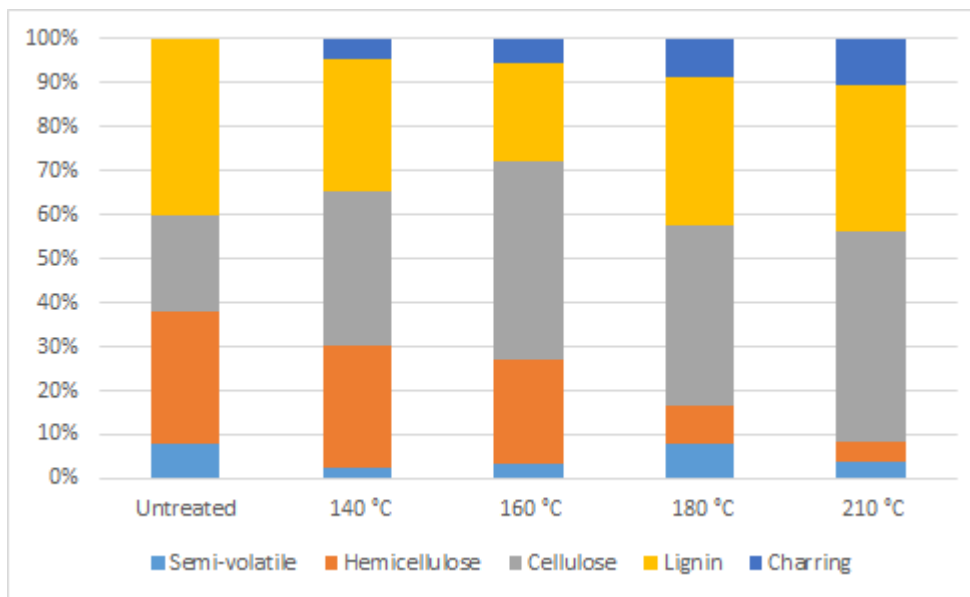


Figure 21: Percent composition of 20 mL/min flow rate at varying temperatures.

Semi-volatile component percentages did not experience significant changes according to our TGA analysis. The compounds compose a small part of the sample and their percentage slightly change at the varying temperature conditions. A possible explanation is that the mass percentage of semi-volatile components was too small to notice a large difference or that the temperature range tested does not have an important effect on these compounds.

The lignin and cellulose percentages vary at the different treatment temperatures with a general increase in mass percentage as temperature increases. This was difficult to quantify because the curves for lignin and cellulose were very close in range and may have interfered with each other. Therefore, it is best to combine the two components and study the trends of the two together. Moreover, char formation was observed at all four temperatures. The char percentage is slightly increases at higher temperatures with the highest value observed at 210°C. As a result, as the temperature rises more char is formed. The highest difference occurs from 160°C to 180°C.

Using FTIR to compare the effect of temperature change on the amplitude of the absorbance bands for both flow rates, yielded to comparable results. Starting with the flow rate of 20 mL/min, the spectra can be found on Figure 22 below.

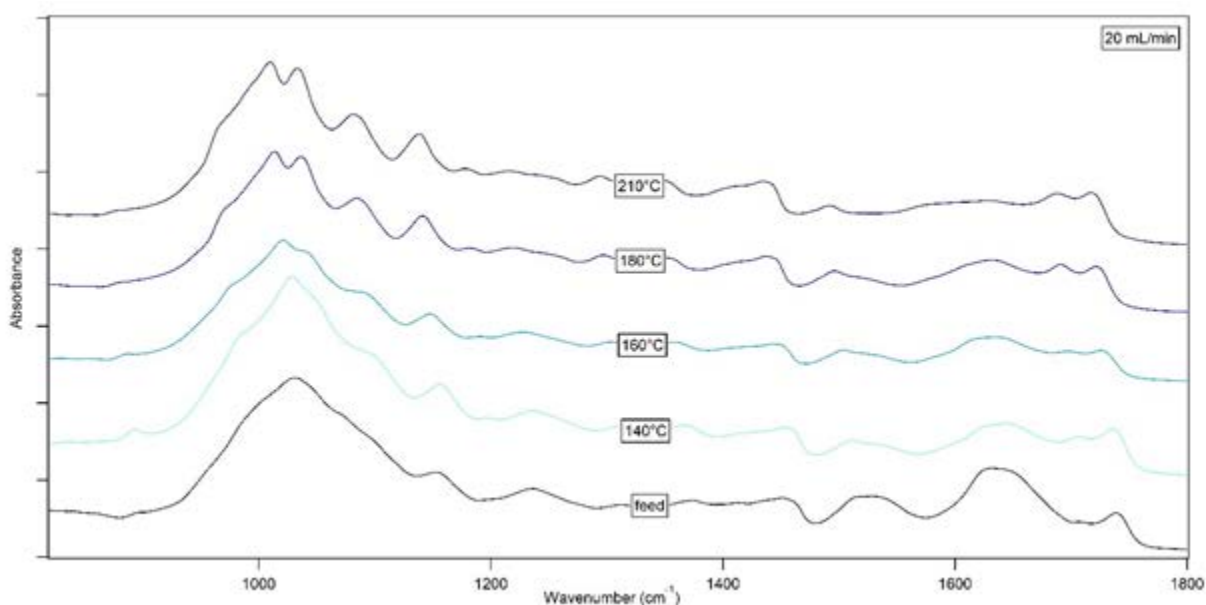


Figure 22: Absorbance spectrum at the 20 mL/min flow rate ( $850\text{cm}^{-1} - 1800\text{cm}^{-1}$ ).

The band that is associated with cellulose in the feed is typically positioned between  $897\text{cm}^{-1}$  and  $910\text{cm}^{-1}$ . For the flowrate of 20 mL/min, the band appears at  $898\text{cm}^{-1}$  and the effect of increasing temperature can be seen by observing the specific peak at different temperatures. As temperature increases, there is a slight shift towards the right and the peak increases until  $160^\circ\text{C}$  when it reaches its maximum and then starts decreasing where it has almost completely disassembled at  $210^\circ\text{C}$ .

The peak appearing at  $1518\text{cm}^{-1}$  represents the presence of lignin. The intensity of the band is kept constant and any change is attributed to overlapping and is considered negligible. This is the reason why lignin is used as a base case in order to compare the change in the peaks of other components. Next, charring can be observed from the peak at  $1710\text{cm}^{-1}$ . We can see that the peak becomes broader as the temperature and intensity increase. The biggest increase can be seen from

160°C to 180°C. This can also be observed by comparing their intensity ratios to lignin, which is considered the base case. The ratio increases from 0.89 at 140°C, to 1.58 at 180°C. This indicates the formation of char in the compound, at higher temperatures of hydrolysis.

Hemicellulose is the most significant compound for our project, since its extraction yields to an increase in biomass material that can be used for the production of biofuels. The peak at 1739  $\text{cm}^{-1}$  is related to hemicellulose. From a first glance it is quite obvious that there is a slight decrease from the untreated feed to 140°C and 160°C accordingly. The large decrease occurs between the temperatures of 160°C and 180°C, with a further decrease at 210 °C, which indicates that at that temperature the maximum amount of hemicellulose has been extracted from the biomass. This means that the samples treated at a higher temperature contain relatively less cellulose, since it has been extracted from the sample as a liquid.

The same patterns as the 20 mL/min were observed for the samples treated at 10 mL/min one. The difference was in the relative amounts. The respective graphs are presented below, Figures 23 and 24. Again, the percentage of hemicellulose reduces with raising temperatures with the greater change from 180 °C to 210 °C, where the percentage drops from 15.08% to 8.18%. The rest of the components follow the same trends with the 20 mL/min results.

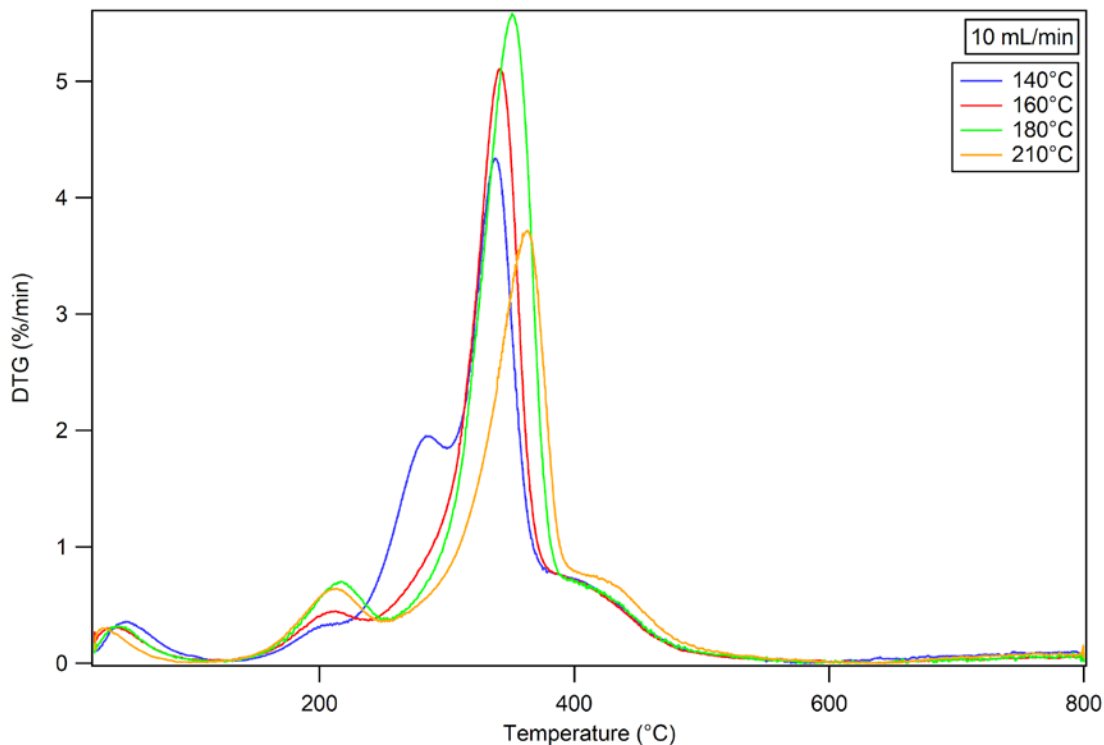


Figure 23: DTG comparisons of treatment temperatures at the 10 mL/min flow rate.

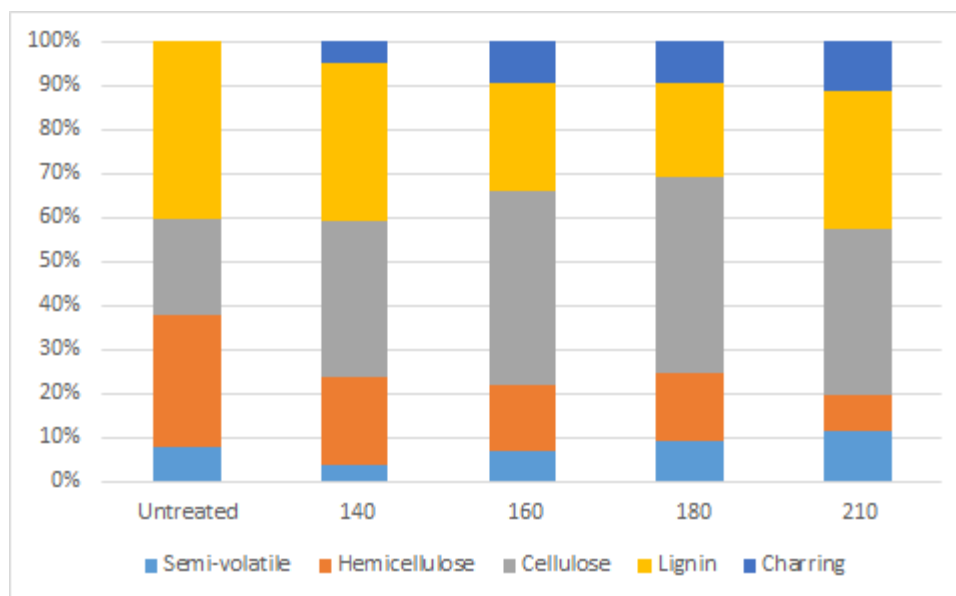


Figure 24: Percent composition of 10 mL/min flow rate at varying temperatures.

We also examined the effect of a range of temperature to the peaks of the FTIR spectra, representing the same components described previously. The trends followed were all the same as the ones mentioned above for the flow rate of 20 mL/min. More specifically, the intensity of the peak representing cellulose initially increases and then starts decreasing until it almost completely disassembles at the temperature of 210 °C, as shown on Figure 25. Lignin is observed to be kept constant, charring increases with increasing temperature, whereas hemicellulose overall decreases with increasing temperature, indicating that there has been greater extraction.

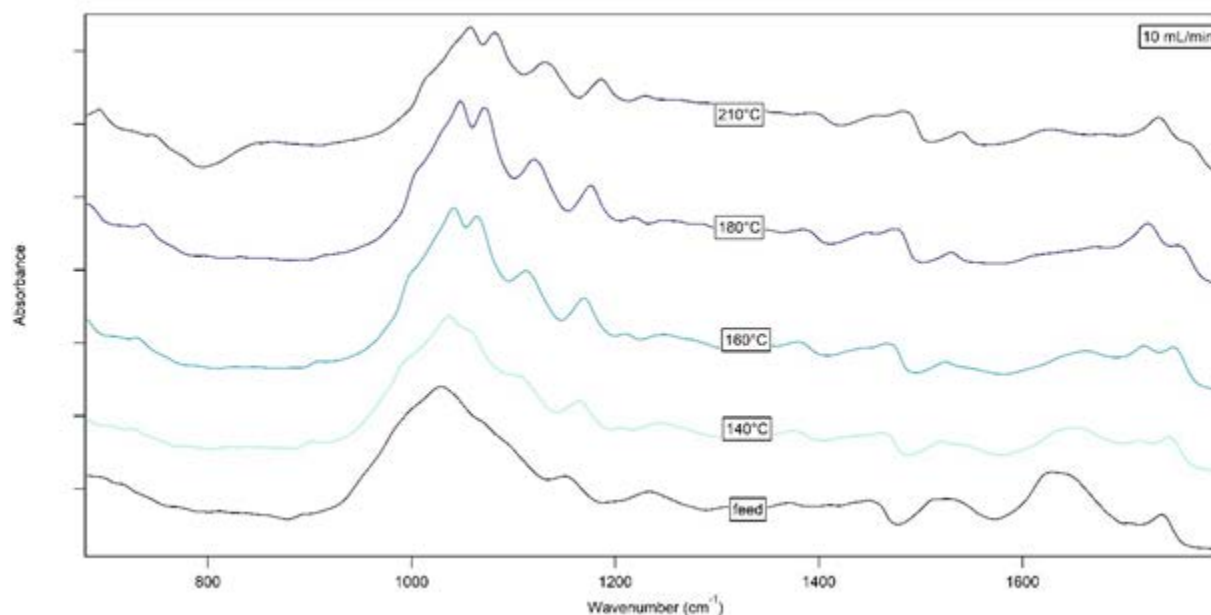


Figure 25: Absorbance spectrum at the 10 mL/min flow rate ( $700\text{cm}^{-1}$  -  $1800\text{cm}^{-1}$ ).

Similar trends were obtained by analyzing the liquid samples in Brazil. Comparisons of the different temperatures for both flow rates are seen in Figure 26. In both cases, the yield of total carbohydrates increases with increasing temperatures. More specifically and as already predicted from TGA analysis, the most significant difference occurs between 160°C and 180°C.

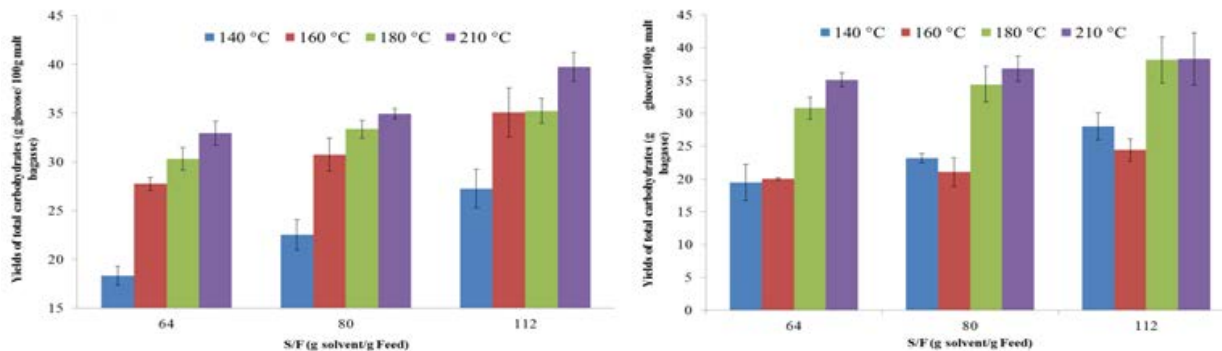


Figure 26: The yield of reducing sugars at different S/F as Temperature changes, retrieved from [59].

The batch process follows the same motif. Figure 27 shows that amplitude of the hemicellulose curve at about 280°C decreases, and also the amplitude of the cellulose peak at about 350°C increases. Additionally, when analyzing the liquid samples that were collected from the batch trials, there was an increase in sugars as the experimental temperature increased.

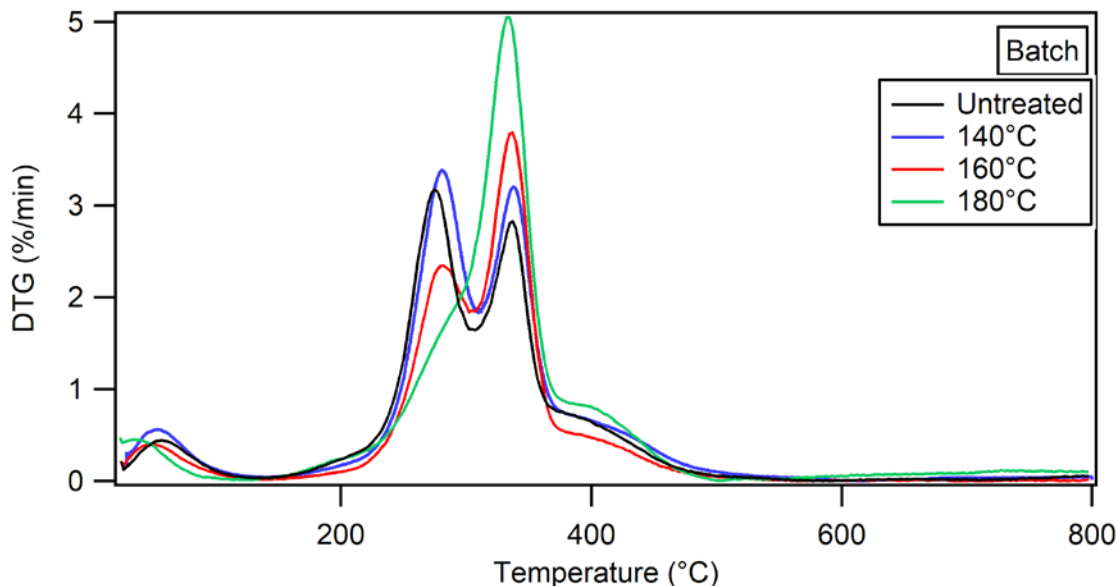


Figure 27: DTG comparisons of treatment temperatures using the batch method.

## 5. Conclusions

After a series of experiments, we were able to determine the optimal treatment conditions of malt bagasse that allows for greater sugar extraction. The highest sugar extraction was seen from the malt bagasse sample that was treated at 210°C at the 20 mL/min flow rate using the flow through process. The most easily recognizable conclusion was the significant difference of extraction from the flow through method versus the batch reaction method. At 140°C, 160°C, and 180°C, the flow through method was more effective than the batch method, and even though we were unable to treat the samples using the batch method at 210 °C, we can predict that the flow through process would be more efficient in this extraction as well. Temperature significantly affected the quantity of hemicellulose extracted, with the most extraction achieved at 210°C. This was important in the determination of which flow rate was optimal, seeing as at the high temperature of 210 °C, the 20 mL/min flow rate was best at sugar extraction.

## 6. Recommendations

To further study the effects of temperature, flow rate, and method of sugar extraction from malt bagasse samples, it is recommended to analyze at least three trials of each sample using thermogravimetric analysis (TGA) and Fourier Transform Infrared Spectroscopy (FTIR). Additional samples and analysis would provide a more confident conclusion on results found from the samples. With a single sample analyzed from each flow rate and temperature, outlying information was not able to be recognized.

During TGA, the mass of malt bagasse was analyzed at temperatures ranging from 25°C to 800°C increasing by intervals of 5°C. The small intervals resulted in many data points, leading to a very large process time for the TGA machine. In a time restricted environment, it is recommended to recalculate the interval size on the machine in order to reduce the experimental time. This would allow for more trials to be done in a shorter amount of time, getting more data points to get a more accurate result.

During experimentation with the batch process for sugar extraction, only temperatures of 140°C, 160°C, and 180°C were tested due to equipment that was unable to handle 210°C. In order to accurately compare the batch process to the flow through treatment, finding materials that would withstand all four temperatures of testing would allow for a better comparison. Additionally, treating the malt bagasse at more temperatures would lead to better data. We recommend having five degree interval sizes, or smaller if possible. Specifically, both the 180°C and 210°C were able to extract sugar efficiently, and the most ideal temperature may be in this range so further testing is necessary.

In addition to a larger range of temperature treatments, looking further into the acid production during the hydrolysis of the sample would provide insight as to why at lower temperatures the lower flow rate is ideal and higher temperatures had more extraction with the higher flow rate. While there is not an answer currently as to why this occurred, studying the byproducts of this experiment may give information on the reactions that occurred in the treatment of the malt bagasse and may be able to provide answers to this question

Another way to improve the comparison of the two processes would be to have the exact amounts of water and sample used in both the batch and flow through techniques. Due to a small sample size, we were unable to keep the correct amounts of sample and water for each trial and instead scaled down the reaction using the same water to sample ratio. We made the assumption that experiment size did not play an impact in sugar extraction, but eliminating this variable would provide more precise data.

During our analysis, FTIR proved to be a challenging instrument for our experiment. Due to the sensitive nature of FTIR, the atmospheric conditions around the machine had the potential to impact the data collected. Moisture in the air or dust particles could have played a roll in incorrect data. Additionally, the graphs generated were difficult to fit due to the constant overlap of peaks that were formed and impacted by multiple compounds. This caused confusion in determining amounts of each compound in the sample, as it was difficult to distinguish. The initial

plan was to fit all the peaks and determine the areas and intensities for each major compound. However, we ended up using general trends observed as temperature and flow rate were varied, meaning how one variable changes as the other ones stay constant. We recommend that a different system of analysis is chosen instead of FTIR for these reasons. If that change is not possible, it is recommended that the FTIR machine is kept in an isolated location to control the amount of variables in the room.

## 7. References

1. Agarwal, U. P. (1999). "An overview of Raman spectroscopy as applied to lignocellulosic materials," in *Advances in Lignocellulosics Characterization*, Chap. 9. ed. D. S. Argyropoulos (Atlanta, GA: TAPPI Press), 201–225.
2. Akhtar, J., & Amin, N. A. S. (2011). A review on process conditions for optimum bio-oil yield in hydrothermal liquefaction of biomass. *Renewable and Sustainable Energy Reviews*, 15(3), 1615-1624.
3. Balat, H., & Balat, M. (2009). Recent trends in global production and utilization of bio-ethanol fuel. *Applied Energy*, 86(11), 2273-2282.
4. Basu, P. (2010). *Biomass gasification and pyrolysis*. Amsterdam: Elsevier, 27-63.
5. Bulkowska, K. (Ed.), Pawlowski, A. (Ed.), Gusiatin, Z. (Ed.), Klimiuk, E. (Ed.), Pokoj, T. (Ed.). (2017). *Biomass for Biofuels*. London: CRC Press.
6. Cai, J., Wu, W., Liu, R., & Huber, G. W. (2013). A distributed activation energy model for the pyrolysis of lignocellulosic biomass. *Green Chemistry*, 15(5), 1331-1340.
7. Cardona, C. A. (2007). Fuel ethanol production: Process design trends and integration opportunities. *Bioresource Technology*, 98(12), 2415-2457.
8. Coleman-Jensen, A., Nord, M., & Singh, A. (2013). Household food security in the United States in 2011.
9. Coseri, S. (2017). Cellulose: To depolymerize... or not to? *Biotechnology Advances*, 35(2), 251-266. doi:10.1016/j.biotechadv.2017.01.002
10. Czernik, S., & Bridgwater, A. V. (2004). Overview of applications of biomass fast pyrolysis oil. *Energy and Fuels*, 18(2), 590-598.
11. Demirbas, A., & Ozturk, T. (2005). Anaerobic digestion of agricultural solid residues. *International Journal of Green Energy*, 1(4), 483-494.
12. Department of Environmental Protection. (2016). Biodiesel. Retrieved from [http://www.ct.gov/deep/cwp/view.asp?a=2708&q=323870&deepNav\\_GID=1763](http://www.ct.gov/deep/cwp/view.asp?a=2708&q=323870&deepNav_GID=1763)
13. Dung, T. N. B., Sen, B., Chen, C. C., Kumar, G., & Lin, C. Y. (2014). Food waste to bioenergy via anaerobic processes. *Energy Procedia*, 61, 307-312.
14. FAO. (2014). Technical platform on the measurement and reduction of food loss and waste. Retrieved from <http://www.fao.org/platform-food-loss-waste/food-waste/definition/en/>

15. Fisher, T., Hajaligol, M., Waymack, B., & Kellogg, D. (2002). Pyrolysis behavior and kinetics of biomass derived materials. *Journal of analytical and applied pyrolysis*, 62(2), 331-349.
16. Girotto, F., Alibardi, L., & Cossu, R. (2015). Food waste generation and industrial uses: A review. *Waste Management*
17. Gunders, D. (2012). *Wasted: How America is losing up to 40 percent of its food from farm to fork to landfill*. Natural Resources Defense Council.
18. Gustavsson, J., Cederberg, C., Sonesson, U., Van Otterdijk, R., & Meybeck, A. (2011). *Global food losses and food waste* (pp. 1-38). Rome: FAO.
19. Haas, M. J., McAloon, A. J., Yee, W. C., & Foglia, T. A. (2006). A process model to estimate biodiesel production costs. *Bioresource Technology*, 97(4), 671-678.
20. Hess, J. R., Wright, C. T., & Kenney, K. L. (2007). Cellulosic biomass feedstocks and logistics for ethanol production. *Biofuels, Bioproducts and Biorefining*, 1(3), 181-190.
21. Hiç, C., Pradhan, P., Rybski, D., & Kropp, J. P. (2016). Food surplus and its climate burdens. *Environmental science & technology*, 50(8), 4269-4277.
22. Huang, G., Chen, F., Chen, G., Wei, D., & Zhang, X. (2009). Biodiesel production by microalgal biotechnology. *Applied Energy*, 87(1), 38-46.
23. Iodice, P., Senatore, A., Langella, G., & Amoresano, A. (2017). Advantages of ethanol-gasoline blends as fuel substitute for last generation si engines. *Environmental Progress & Sustainable Energy*, 36(4), 1173-1179.
24. Jalvandi, J. (2016). Novel chemical and physical approaches for sustainable drug release from biodegradable electrospun nanofibers.
25. Jessop, P. G., & Leitner, W. (1999). *Supercritical fluids as media for chemical reactions*. *Chemical Synthesis Using Supercritical Fluids*, 1-36.
26. Jose, S., & Bhaskar, T. (Eds.). (2015). *Biomass and biofuels: advanced biorefineries for sustainable production and distribution*. CRC Press.
27. Kacurikova, M., Wellner, N., Ebringerova, A., Hromidkova, Z., Wilson, R. H., and Belton, P. S. (1998). Characterization of xylan-type polysaccharides and associated cell wall components by FT-IR and FT-Raman spectroscopies. *Food Hydrocoll.* 13, 35-41.
28. Kiran, E. U., Trzcinski, A. P., Ng, W. J., & Liu, Y. (2014). Bioconversion of food waste to energy: a review. *Fuel*, 134, 389-399.

29. Klemm, D., Heublein, B., Fink, H. P., & Bohn, A. (2005). Cellulose: fascinating biopolymer and sustainable raw material. *Angewandte Chemie International Edition*, 44(22), 3358-3393.
30. Kusdiana, D., & Saka, S. (2001). Kinetics of transesterification in rapeseed oil to biodiesel fuel as treated in supercritical methanol. *Fuel*, 80(5), 693-698.
31. Lee, R. A., & Lavoie, J. M. (2013). From first-to third-generation biofuels: Challenges of producing a commodity from a biomass of increasing complexity. *Animal Frontiers*, 3(2), 6-11.
32. Liew, W. H., Hassim, M. H., & Ng, D. K. (2014). Review of evolution, technology and sustainability assessments of biofuel production. *Journal of Cleaner Production*, 71, 11-29.
33. Liew, L. N., Shi, J., & Li, Y. (2012). Methane production from solid-state anaerobic digestion of lignocellulosic biomass. *Biomass and Bioenergy*, 46, 125-132.
34. Lin, C. S. K., Pfaltzgraff, L. A., Herrero-Davila, L., Mubofu, E. B., Abderrahim, S., Clark, J. H., ... & Thankappan, S. (2013). Food waste as a valuable resource for the production of chemicals, materials and fuels. Current situation and global perspective. *Energy & Environmental Science*, 6(2), 426-464.
35. Lissens, G., Verstraete, W., Albrecht, T., Brunner, G., Creuly, C., Seon, J., ... & Lasseur, C. (2004). Advanced anaerobic bioconversion of lignocellulosic waste for bioregenerative life support following thermal water treatment and biodegradation by *Fibrobacter succinogenes*. *Biodegradation*, 15(3), 173-183.
36. Lu, F., & Ralph, J. (2010). Chapter 6-Lignin, Cereal Straw as a Resource for Sustainable Biomaterials and Biofuels. Amsterdam: Elsevier, 169-207.
37. Marchetti, J. M., Miguel, V. U., & Errazu, A. F. (2007). Possible methods for biodiesel production. *Renewable and sustainable energy reviews*, 11(6), 1300-1311.
38. Miller, M. T., & Massey, P. (2016). *The Crime Scene, A Visual Guide*. Retrieved January 25, 2018, from <https://www.sciencedirect.com/science/article/pii/B9780128012451000086>
39. Mohan, D., Pittman, C. U., & Steele, P. H. (2006). Pyrolysis of wood/biomass for bio-oil: a critical review. *Energy & fuels*, 20(3), 848-889.

40. Mothé, C. G., & de Miranda, I. C. (2009). Characterization of sugarcane and coconut fibers by thermal analysis and FTIR. *Journal of Thermal Analysis and Calorimetry*, 97(2), 661.
41. Munir, S., Daood, S. S., Nimmo, W., Cunliffe, A. M., & Gibbs, B. M. (2009). Thermal analysis and devolatilization kinetics of cotton stalk, sugar cane bagasse and shea meal under nitrogen and air atmospheres. *Bioresource Technology*, 100(3), 1413-1418.
42. Nigam, P. S., & Singh, A. (2011). Production of liquid biofuels from renewable resources. *Progress in energy and combustion science*, 37(1), 52-68.
43. Olsen, A. E., & Caruana, D. J. (2012). *Anaerobic digestion: Processes, products, and applications* Nova Science Publishers, Inc.
44. Peng, Y., & Wu, S. (2010). The structural and thermal characteristics of wheat straw hemicellulose. *Journal of Analytical and Applied Pyrolysis*, 88(2), 134-139.
45. Pinnarat, T., & Savage, P. E. (2008). Assessment of noncatalytic biodiesel synthesis using supercritical reaction conditions. *Industrial & Engineering Chemistry Research*, 47(18), 6801-6808.
46. Ragauskas, A. J. (2014). *Materials for biofuels*. New Jersey: World Scientific.
47. Ren, Q., Zhao, C., Chen, X., Duan, L., Li, Y., & Ma, C. (2011). NO<sub>x</sub> and N<sub>2</sub>O precursors (NH<sub>3</sub> and HCN) from biomass pyrolysis: Co-pyrolysis of amino acids and cellulose, hemicellulose and lignin. *Proceedings of the Combustion Institute*, 33(2), 1715-1722. doi:10.1016/j.proci.2010.06.033
48. Schill, S. R. (2008). Sizing up the soybean market. *Biodiesel Mag*.
49. Schulz, H., and Baranska, M. (2007). Identification and quantification of valuable plant substances by IR and Raman spectroscopy. *Vib. Spectrosc.* 43, 13–25.
50. Sims, R. E., Mabee, W., Saddler, J. N., & Taylor, M. (2010). An overview of second generation biofuel technologies. *Bioresource technology*, 101(6), 1570-1580.
51. Spires, T. (2001). Introduction to IR spectroscopy. Retrieved from <https://niu.edu/chembio/pdf/analytical-lab/ftir/FTIR-intro.pdf>
52. Stöcker, M. (2008). Biofuels and biomass-to-liquid fuels in the biorefinery: Catalytic conversion of lignocellulosic biomass using porous materials. *Angewandte Chemie International Edition*, 47(48), 9200-9211.
53. Strezov, V., & Evans, T. J. (Eds.). (2014). *Biomass processing technologies*. CRC Press.

54. Sun, R. (2010). Cereal straw as a resource for sustainable biomaterials and biofuels: chemistry, extractives, lignins, hemicelluloses and cellulose. Amsterdam: Elsevier, 73-130.
55. Taylor, R., Natrass, L., Alberts, G., Robson, P., Chudziak, C., Bauen, A., . . . Ree, v., R. (2015). From the sugar platform to biofuels and biochemicals: Final report for the european commission directorate-general energy. E4tech/Re-CORD/Wageningen UR. Retrieved from <http://www.narcis.nl/publication/RecordID/oai:library.wur.nl:wurpubs%2F492297>
56. Tekin, K., Karagöz, S., & Bektaş, S. (2014). A review of hydrothermal biomass processing. *Renewable and sustainable Energy reviews*, 40, 673-687.
57. Thi, N. B. D., Kumar, G., & Lin, C. Y. (2015). An overview of food waste management in developing countries: current status and future perspective. *Journal of environmental management*, 157, 220-229.
58. Torres-Mayangaa, P. C., Azambujaa, S. P. H., Tompsett, G. A., Guerra, P., Timko, M. T., Goldbecka, R., . . . Forster-Carneiro, T. Subcritical water hydrolysis of malt bagasse: Selective production of hemicellulosic sugars (C-5 sugars) (To be Published)
59. Types of biofuel. Retrieved from <http://biofuel.org.uk/types-of-biofuels.html>
60. U. S Department of Energy. Biomass resources. Retrieved from <https://www.energy.gov/eere/bioenergy/biomass-resources>
61. U.S Department of Energy. (2018). Ethanol fuel basics. Retrieved from [https://www.afdc.energy.gov/fuels/ethanol\\_fuel\\_basics.html](https://www.afdc.energy.gov/fuels/ethanol_fuel_basics.html)
62. Van Gerpen, J. (2005). Biodiesel processing and production. *Fuel processing technology*, 86(10), 1097-1107.
63. Vassilev, S. V., Baxter, D., Andersen, L. K., Vassileva, C. G., & Morgan, T. J. (2012). An overview of the organic and inorganic phase composition of biomass. *Fuel*, 94, 1-33.
64. Villanueva, M., Proupín, J., Rodríguez-Añón, J. A., Fraga-Grueiro, L., Salgado, J., & Barros, N. (2010). Energetic characterization of forest biomass by calorimetry and thermal analysis. *Journal of thermal analysis and calorimetry*, 104(1), 61-67.
65. Watkins, D., Nuruddin, M., Hosur, M., Tcherbi-Narteh, A., & Jeelani, S. (2015). Extraction and characterization of lignin from different biomass resources. *Journal of Materials Research and Technology*, 4(1), 26-32.
66. Yang, B., & Wyman, C. E. (2008). Pretreatment: the key to unlocking low-cost cellulosic ethanol. *Biofuels, Bioproducts and Biorefining*, 2(1), 26-40.

67. Zhang, Q., Chang, J., Wang, T., & Xu, Y. (2007). Review of biomass pyrolysis oil properties and upgrading research. *Energy conversion and management*, 48(1), 87-92.
68. Zheng, Y., Pan, Z., & Zhang, R. (2009). Overview of biomass pretreatment for cellulosic ethanol production. *International journal of agricultural and biological engineering*, 2(3), 51-68.

# 8. Appendices

## 8.1 Appendix A: FTIR Absorbance Spectra

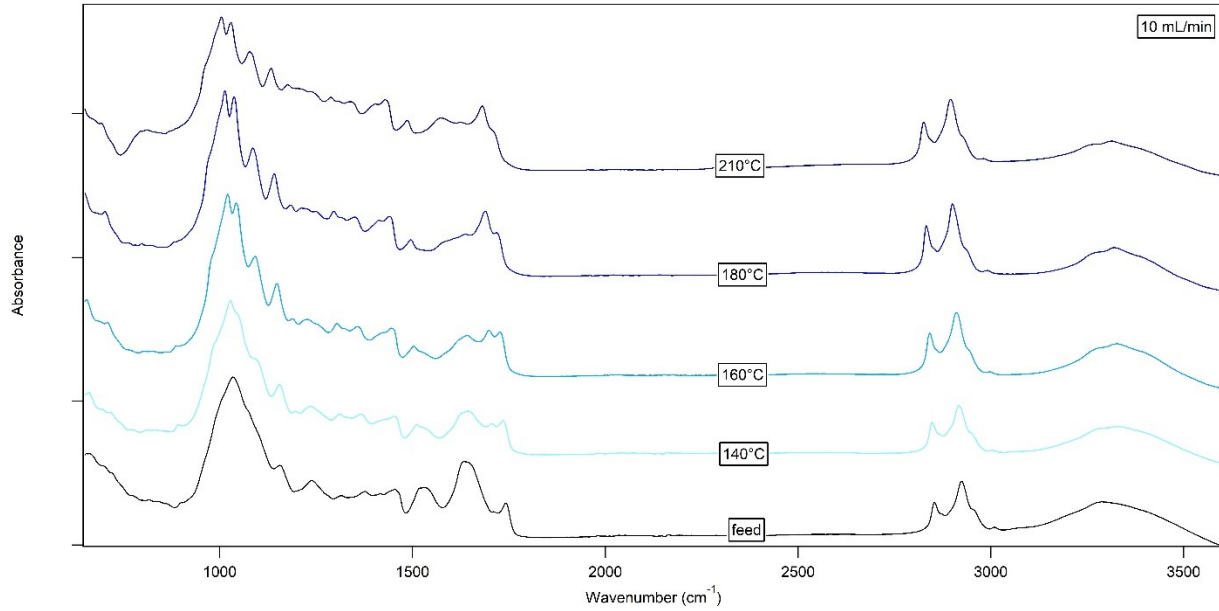


Figure 28: Absorbance spectrum at the 10 mL/min flow rate ( $650\text{cm}^{-1}$  -  $3550\text{cm}^{-1}$ ).

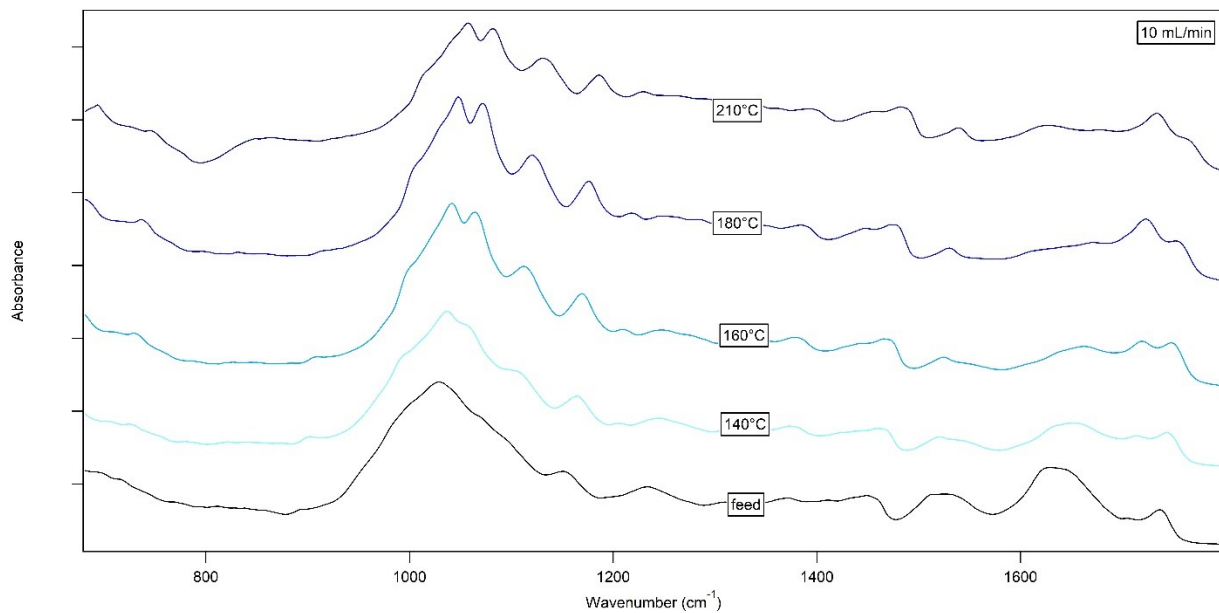


Figure 29: Absorbance spectrum at the 10 mL/min flow rate ( $700\text{cm}^{-1}$  -  $1800\text{cm}^{-1}$ ).

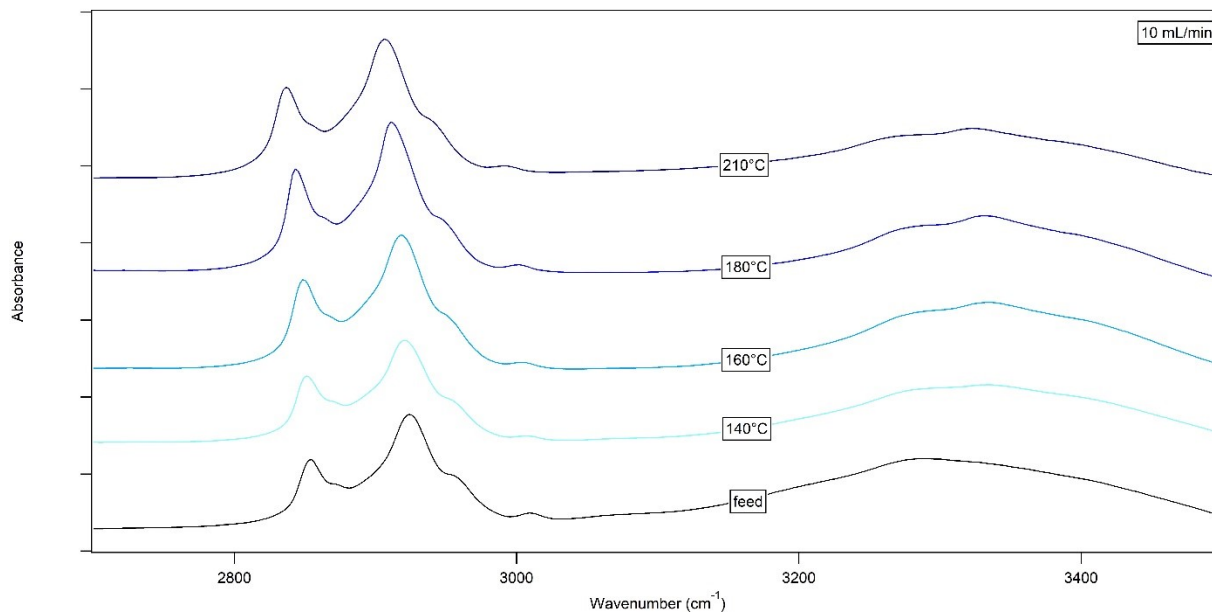


Figure 30: Absorbance spectrum at the 10 mL/min flow rate ( $2600\text{cm}^{-1} - 3550\text{cm}^{-1}$ ).

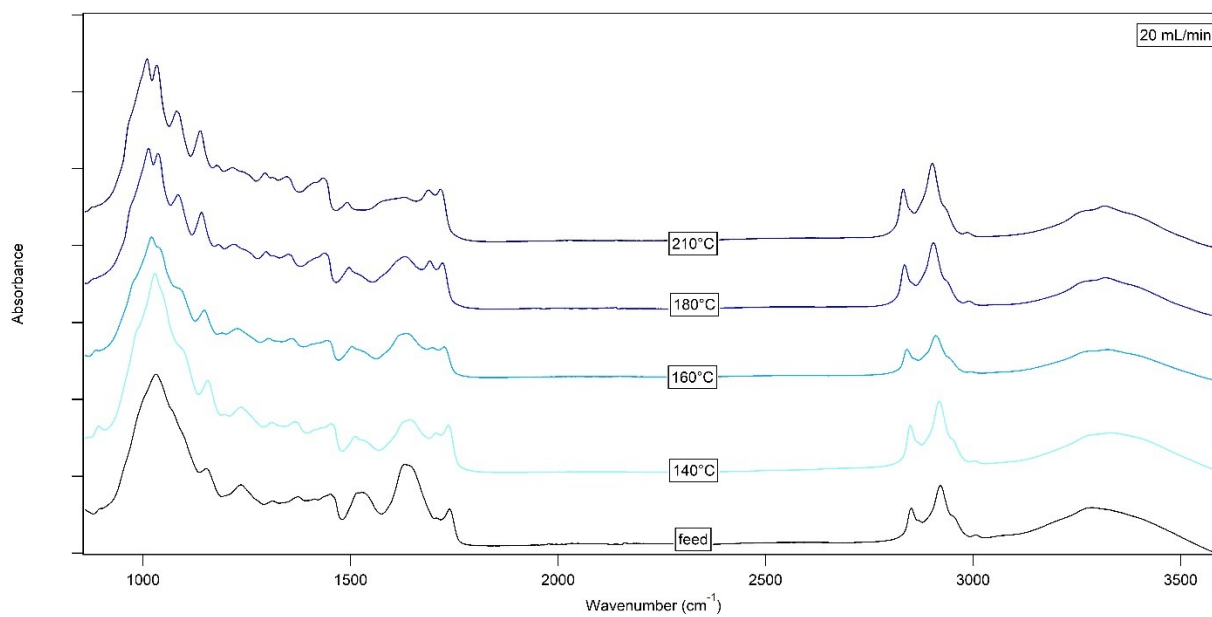


Figure 31: Absorbance spectrum at the 20 mL/min flow rate ( $650\text{cm}^{-1} - 3550\text{cm}^{-1}$ ).

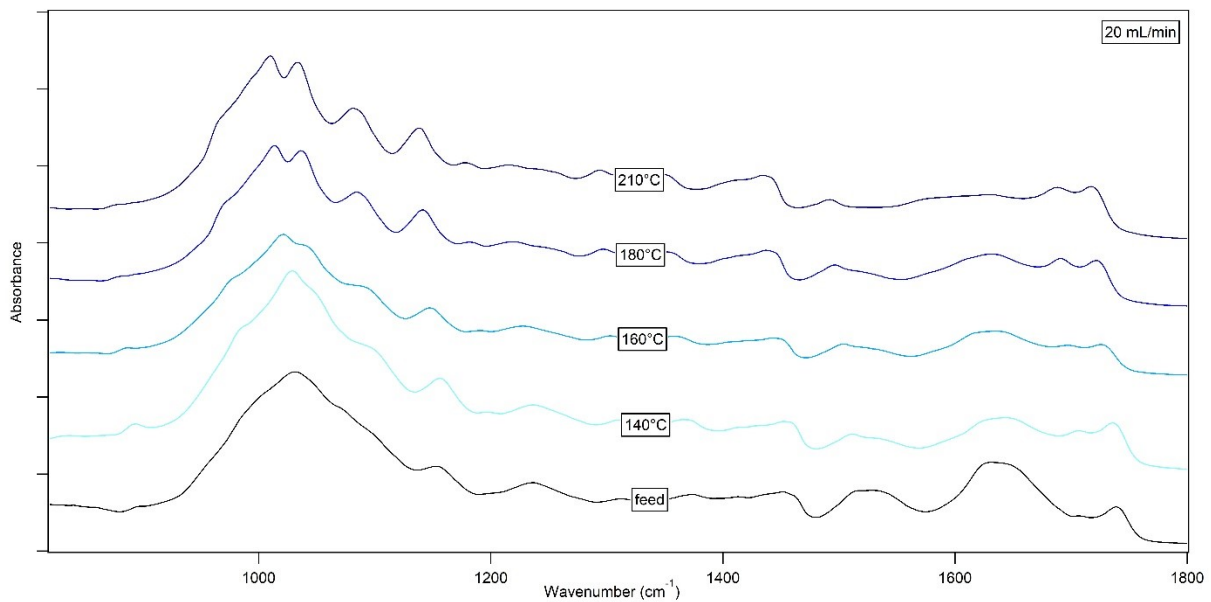


Figure 32: Absorbance spectrum at the 20 mL/min flow rate ( $850\text{cm}^{-1} - 1800\text{cm}^{-1}$ ).

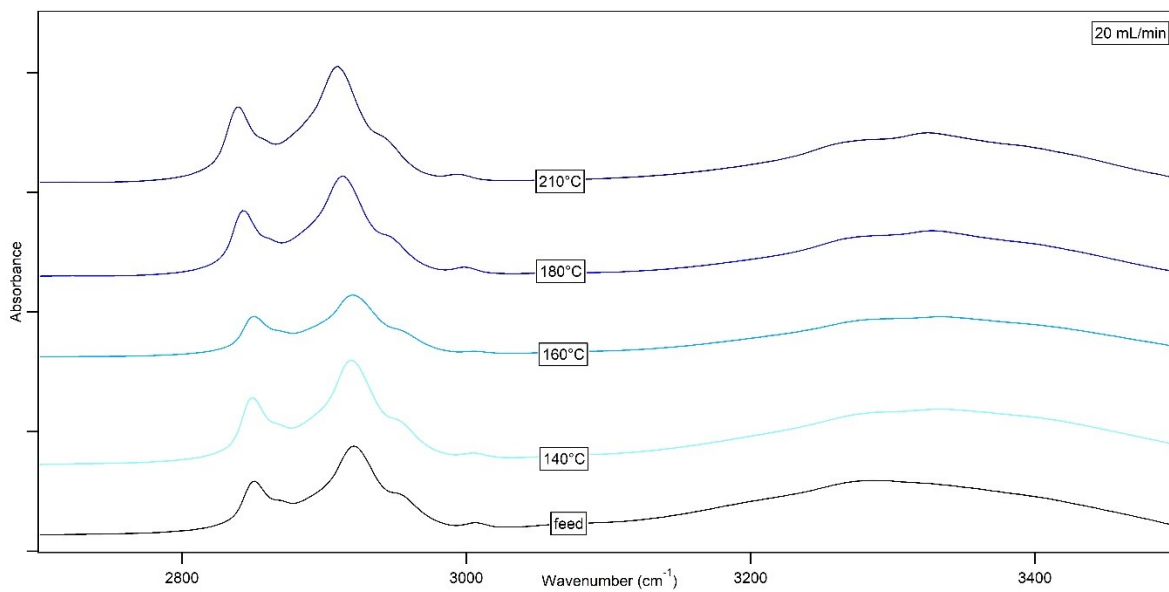


Figure 33: Absorbance spectrum at the 20 mL/min flow rate ( $2600\text{cm}^{-1} - 3550\text{cm}^{-1}$ ).

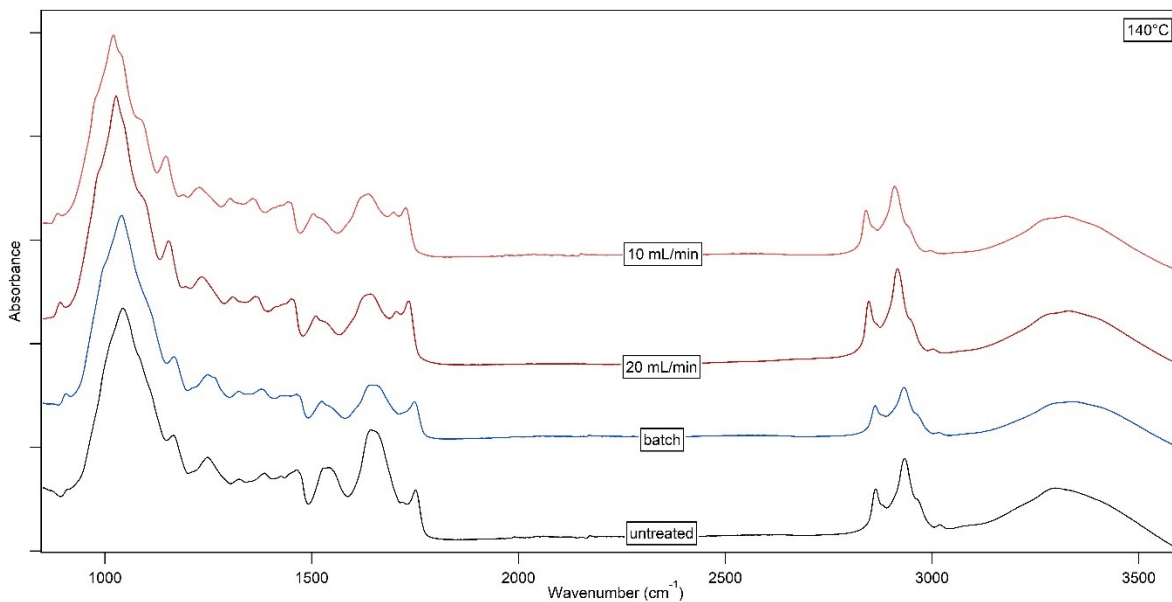


Figure 34: Absorbance spectrum at 140°C (650 $cm^{-1}$  - 3550 $cm^{-1}$ ).

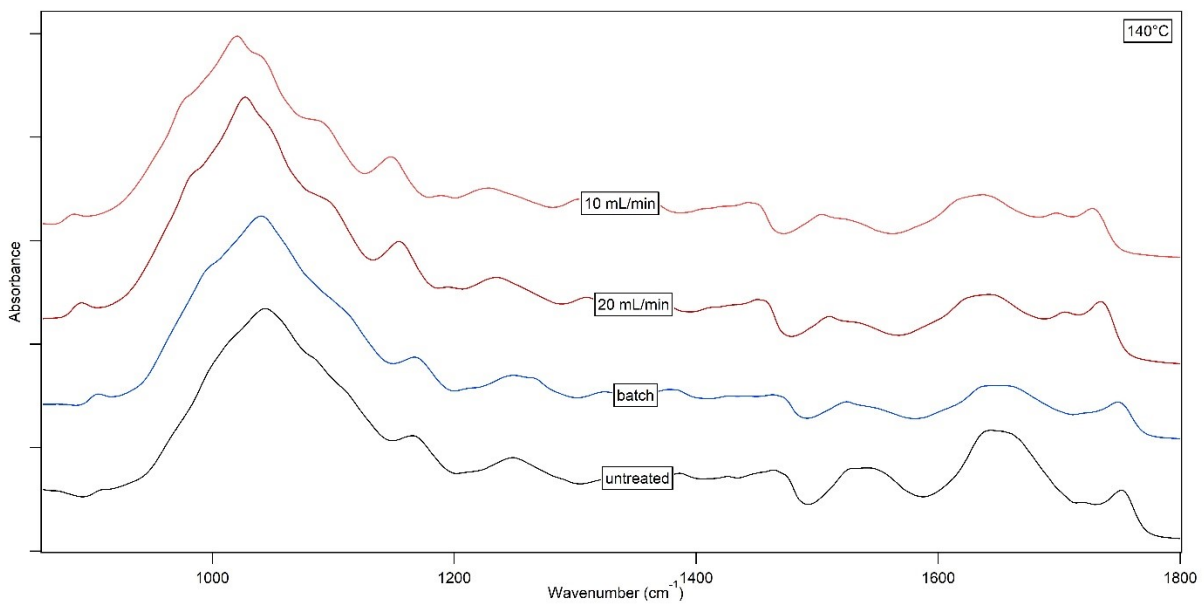


Figure 35: Absorbance spectrum at 140°C (850 $cm^{-1}$  - 1800 $cm^{-1}$ ).

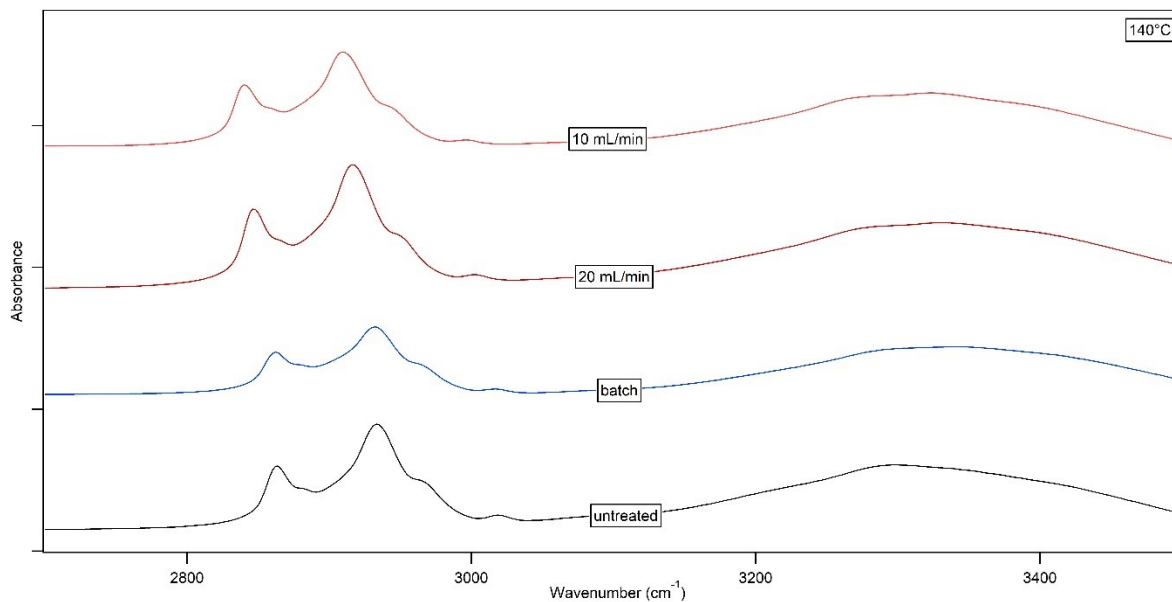


Figure 36: Absorbance spectrum at 140°C ( $2600\text{cm}^{-1}$  -  $3550\text{cm}^{-1}$ ).

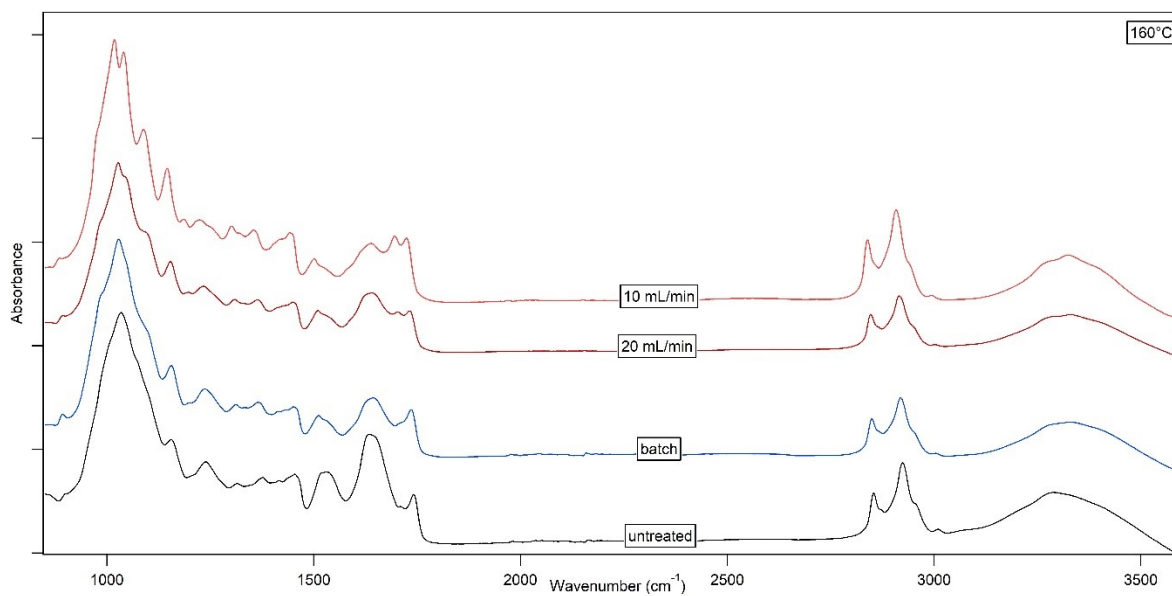


Figure 37: Absorbance spectrum at 160°C ( $650\text{cm}^{-1}$  -  $3550\text{cm}^{-1}$ ).

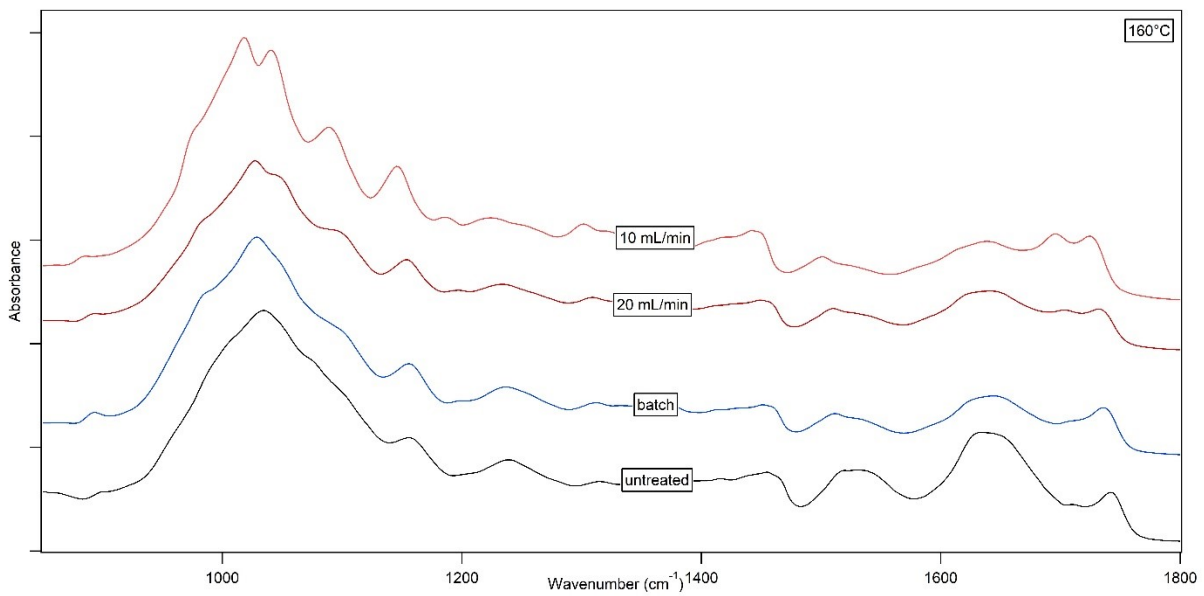


Figure 38: Absorbance spectrum at 160°C (850cm<sup>-1</sup> - 1800cm<sup>-1</sup>).

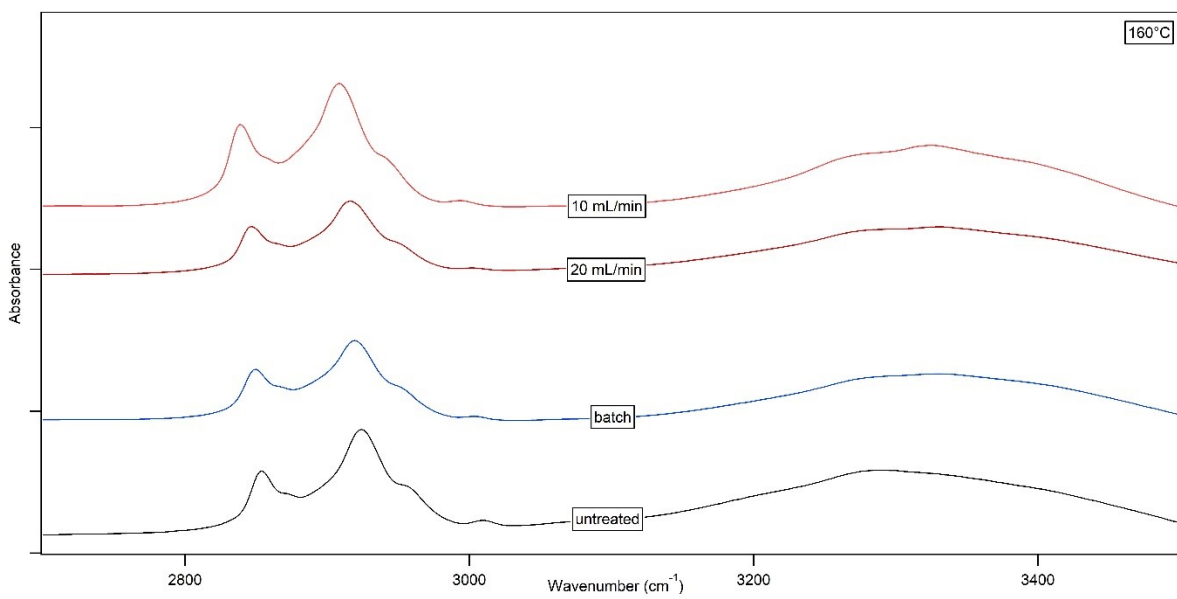


Figure 39: Absorbance spectrum at 160°C (2600cm<sup>-1</sup> - 3500cm<sup>-1</sup>).

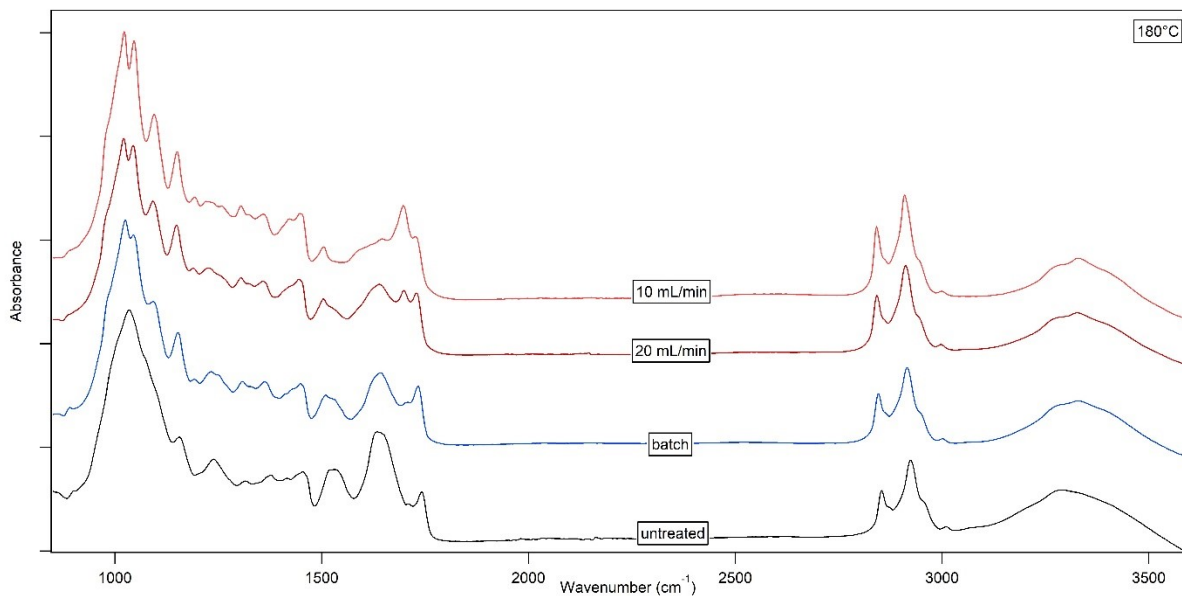


Figure 40: Absorbance spectrum at 180°C (950cm<sup>-1</sup> - 3550cm<sup>-1</sup>).

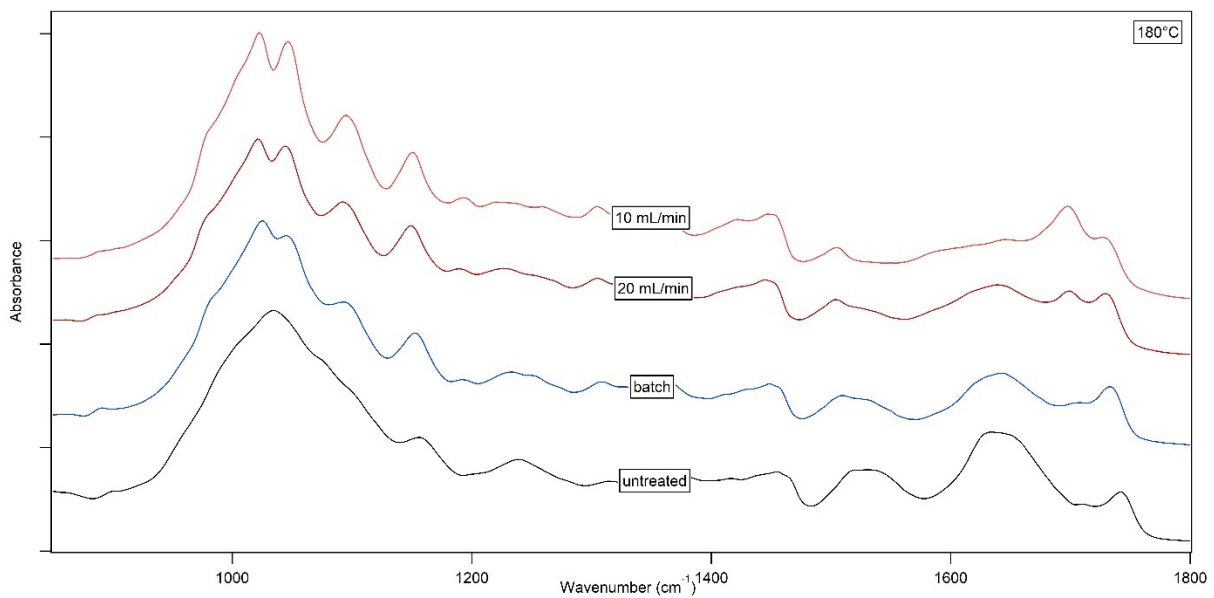


Figure 41: Absorbance spectrum at 180°C (850cm<sup>-1</sup> - 1800cm<sup>-1</sup>).

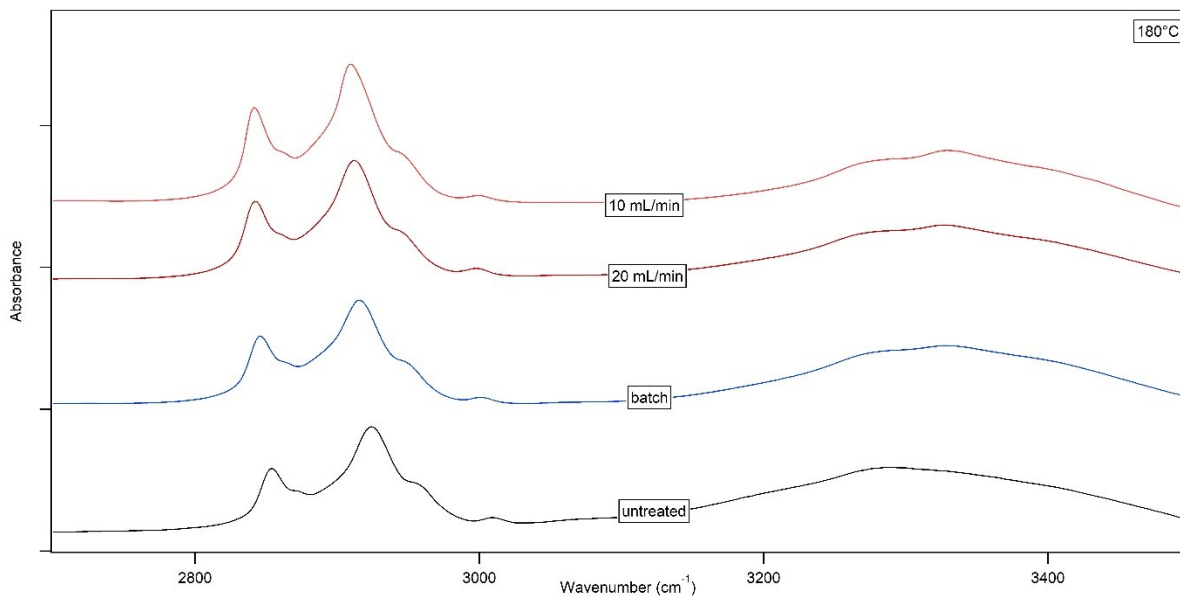


Figure 42: Absorbance spectrum at 180°C (2600 $cm^{-1}$  - 3500 $cm^{-1}$ ).

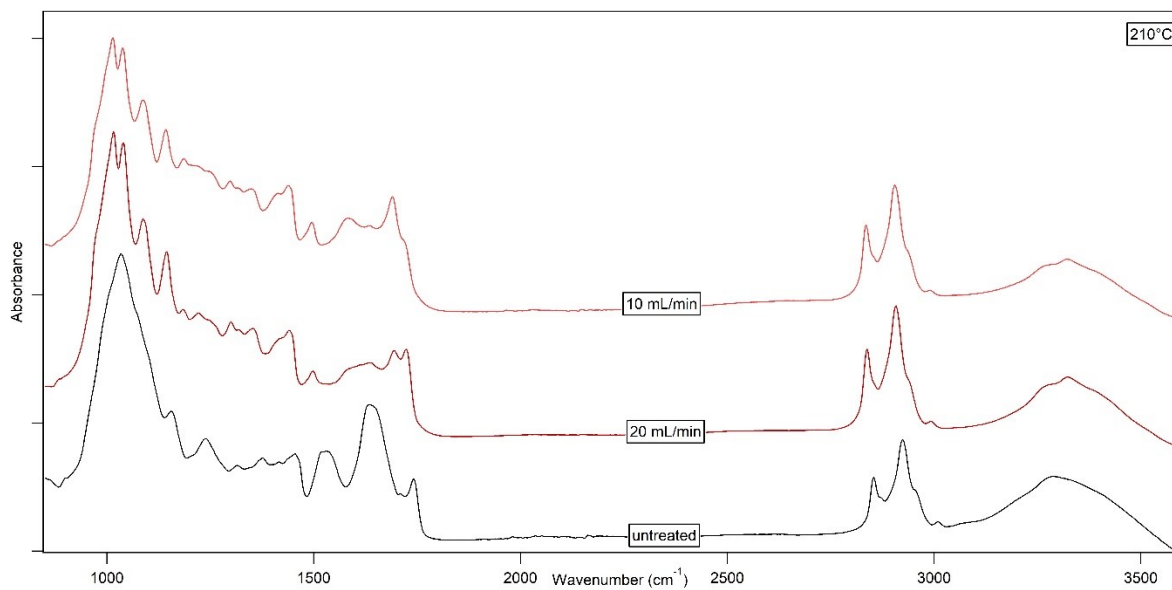


Figure 43: Absorbance spectrum at 210°C (950 $cm^{-1}$  - 3550 $cm^{-1}$ ).

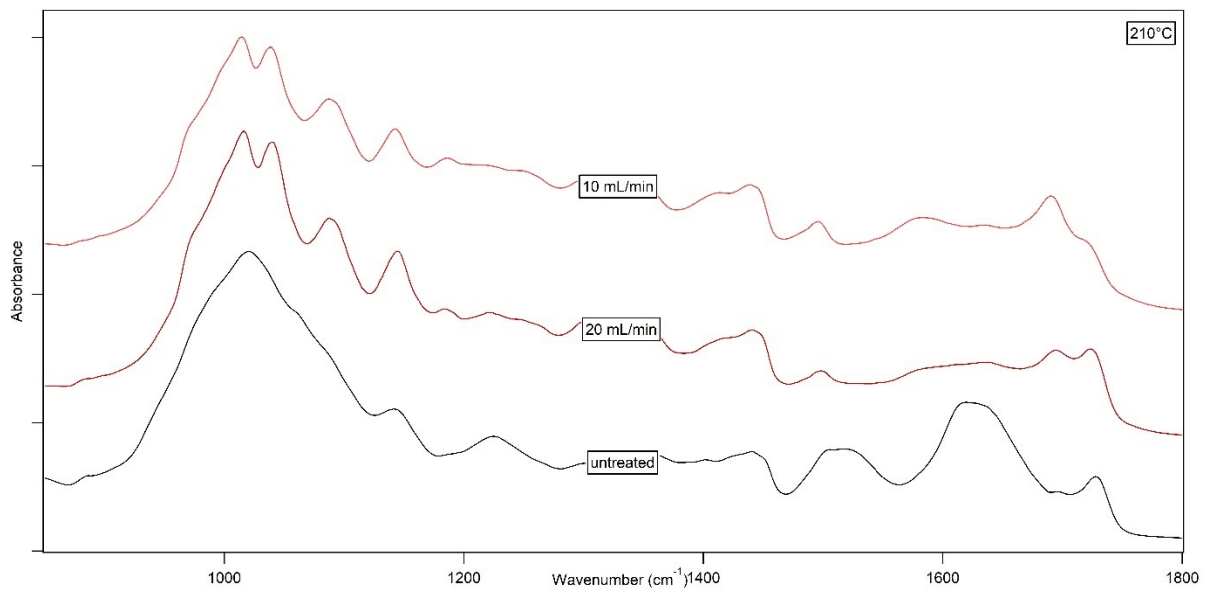


Figure 44: Absorbance spectrum at 210°C (850cm<sup>-1</sup> - 1800cm<sup>-1</sup>).

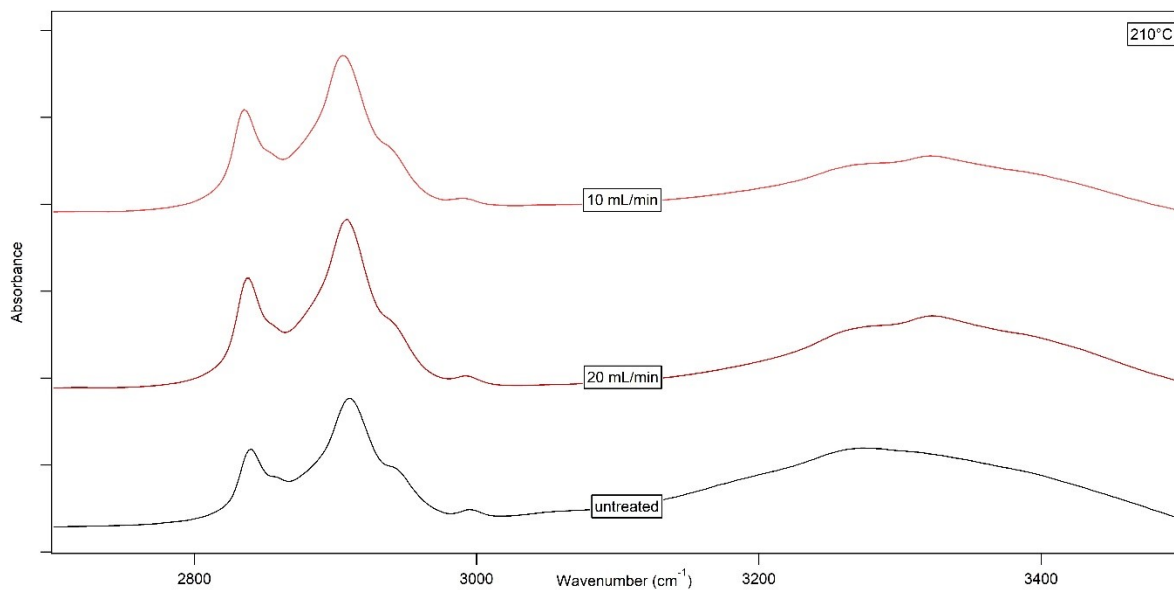


Figure 45: Absorbance spectrum at 210°C (2600cm<sup>-1</sup> - 3500cm<sup>-1</sup>).

## 8.2 Appendix B: TGA Results

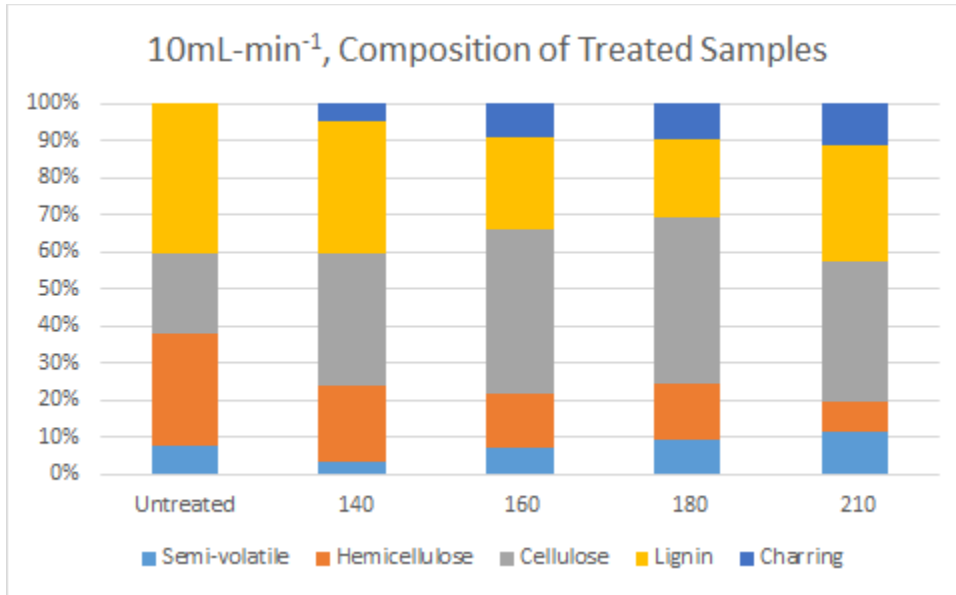


Figure 46: Composition of treated samples at the flow rate of 10 mL/min.

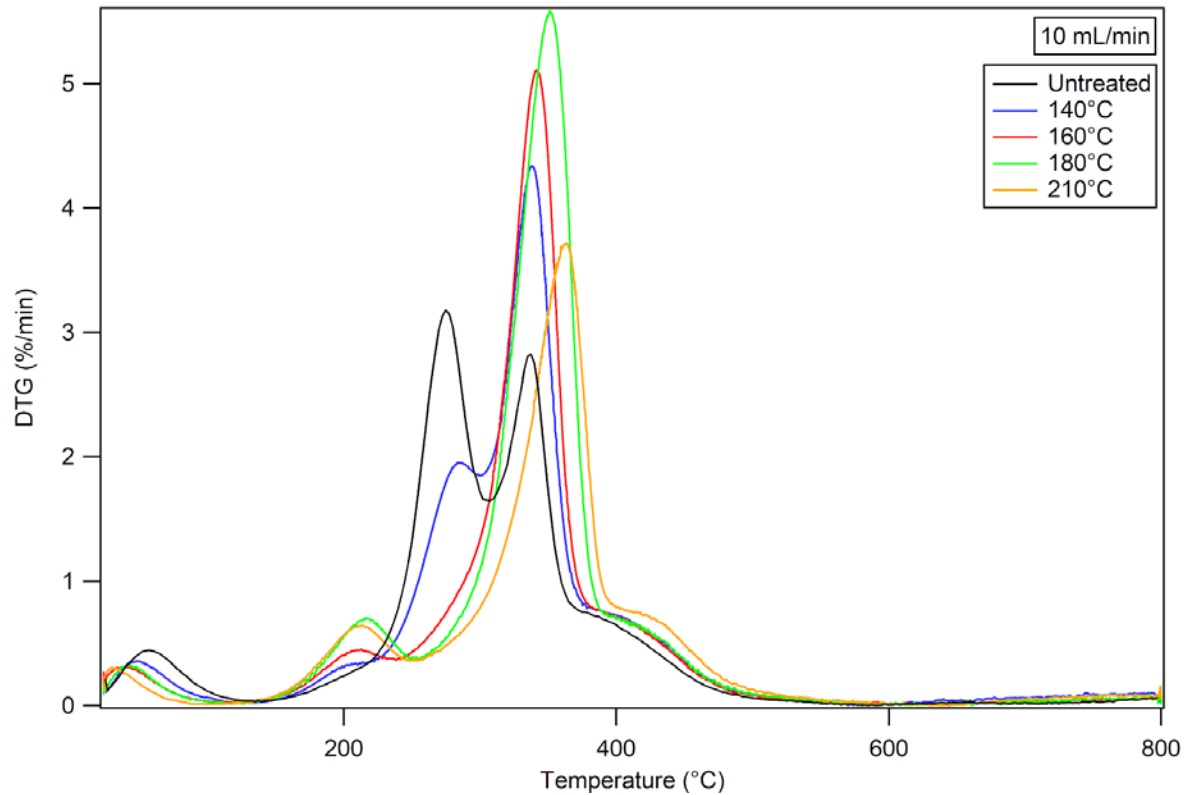


Figure 47: TGA results for untreated feed and treated samples at the flow rate of 10 mL/min.

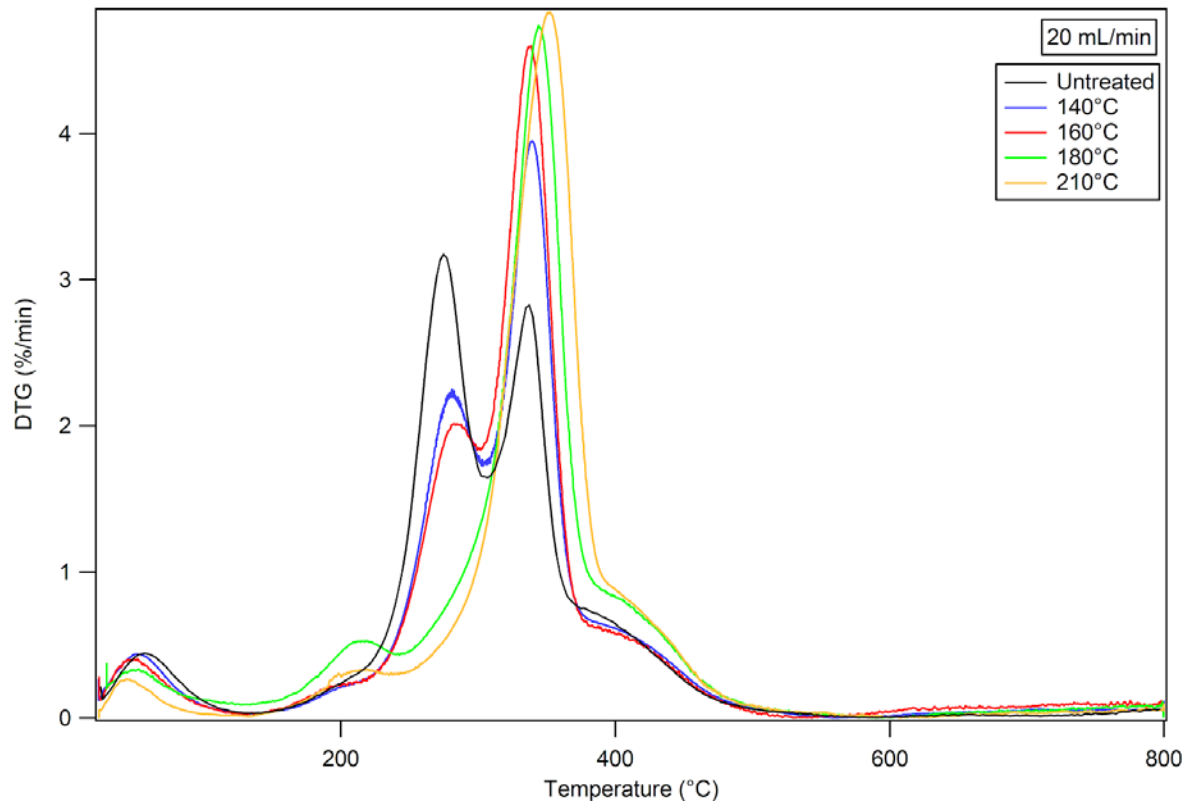


Figure 48: TGA results for untreated feed and treated samples at the flow rate of 20 mL/min.

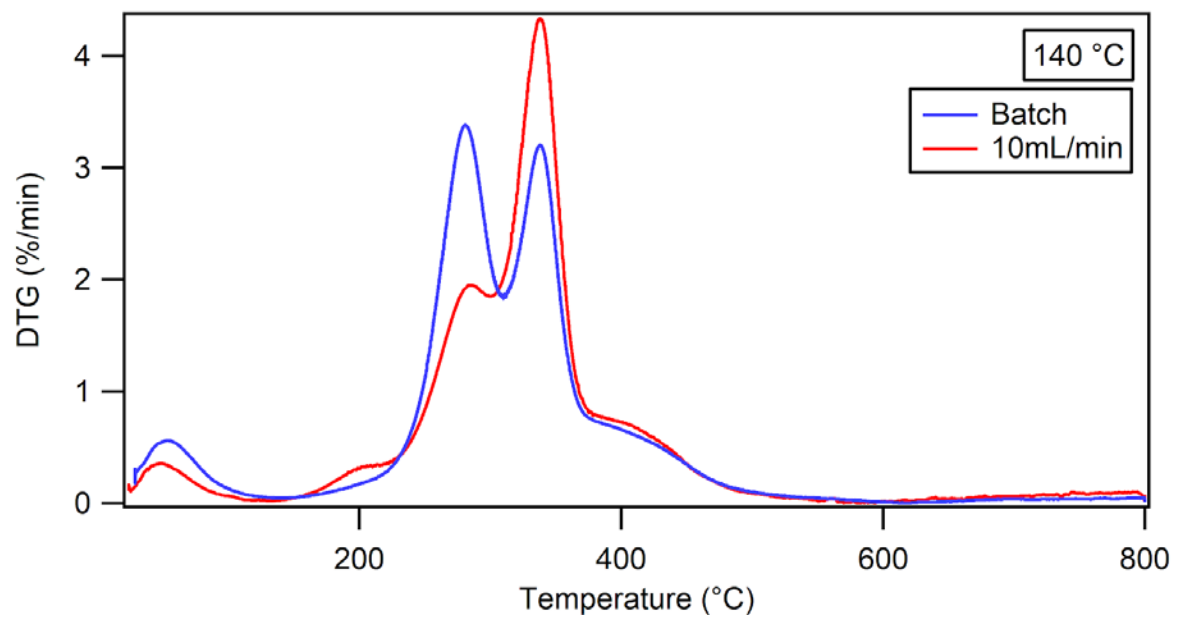


Figure 49: TGA results for treated sample at a flow rate of 10 mL/min and batch experiment at 140°C.

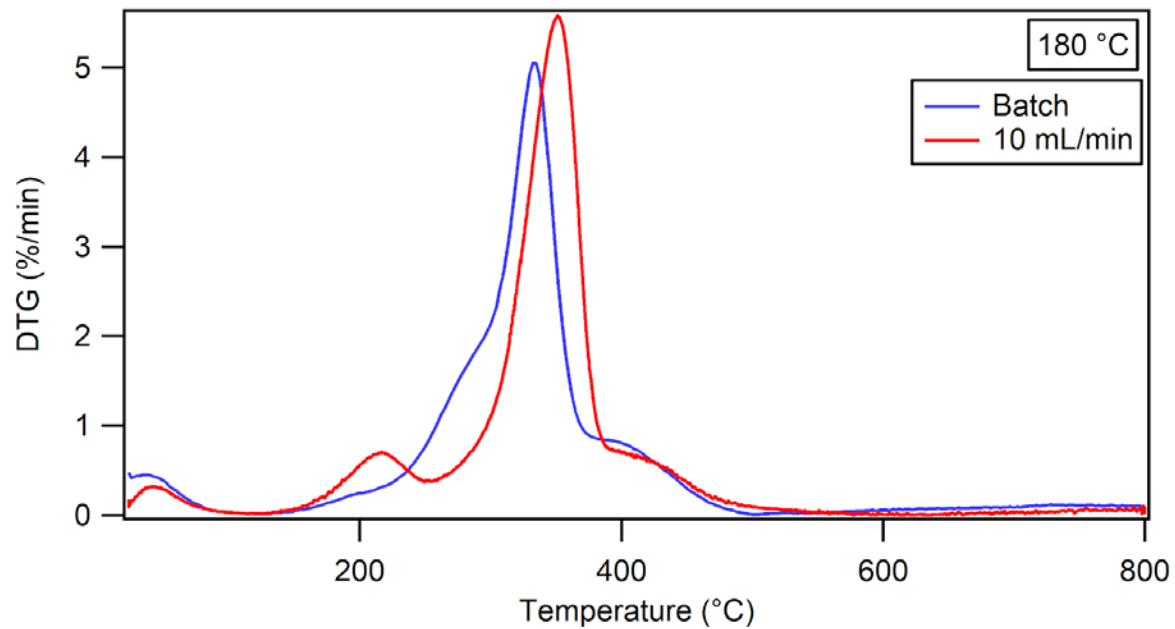


Figure 50: TGA results for treated sample at a flow rate of 10 mL/min and batch experiment at 180°C.

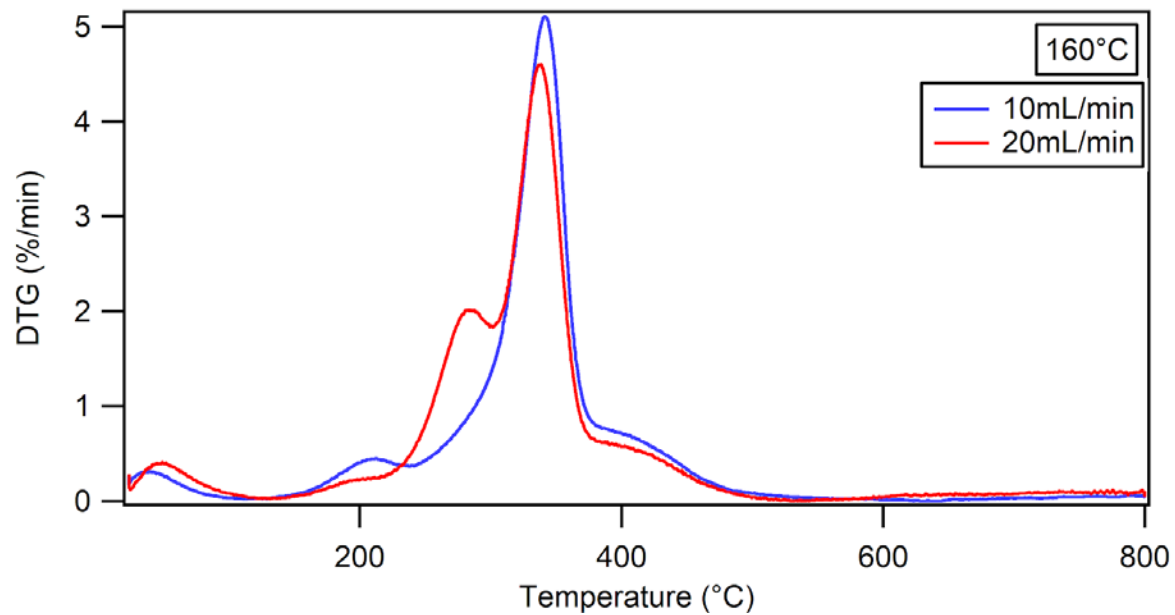


Figure 51: TGA results for treated samples at flow rates of 10 mL/min and 20 mL/min respectively, at 160°C.

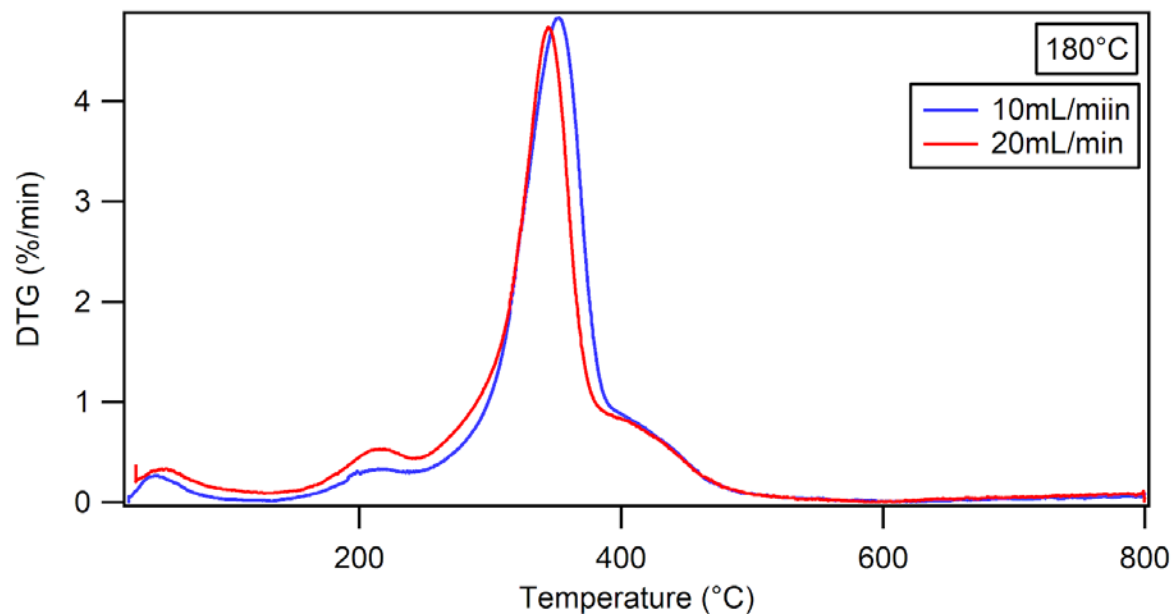


Figure 52: TGA results for treated samples at flow rates of 10 mL/min and 20 mL/min respectively, at 180°C.

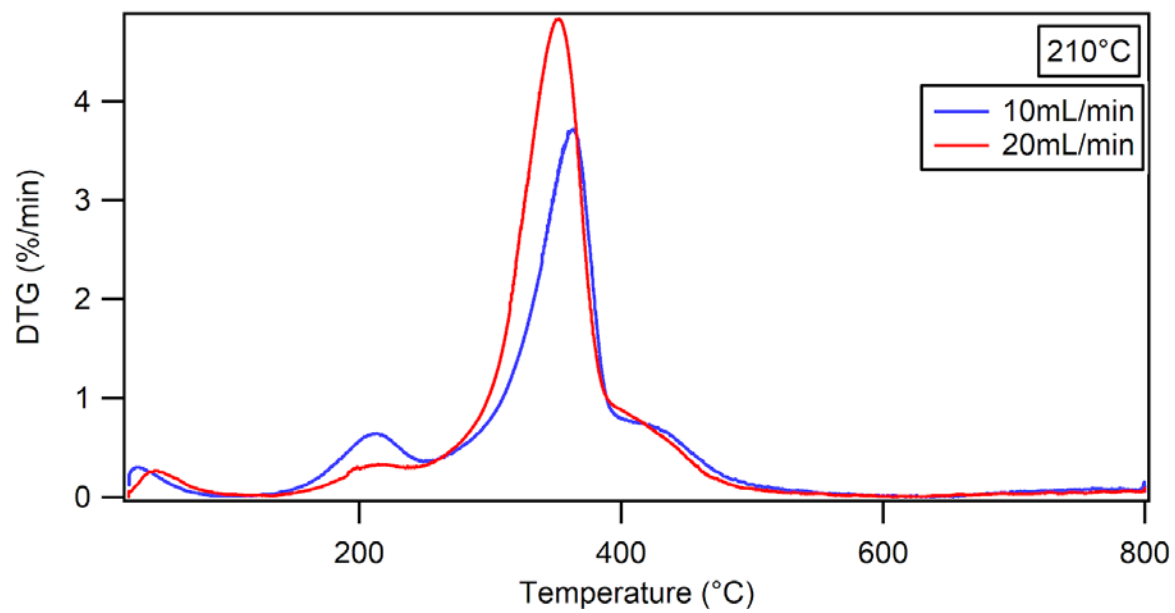


Figure 53: TGA results for treated samples at flow rates of 10 mL/min and 20 mL/min respectively, at 210°C.